



ELSEVIER

Contents lists available at ScienceDirect

Bioorganic Chemistry

journal homepage: www.elsevier.com/locate/bioorg

Synthesis and biological evaluation of novel millepachine derivative containing aminophosphonate ester species as novel anti-tubulin agents

Xiaochao Huang^{a,*}, Meng Wang^{a,1}, Chungu Wang^c, Weiwei Hu^a, Qinghong You^a, Tianhua Ma^d, Qiang Jia^d, Chunhao Yu^a, Zhixin Liao^{c,*}, Hengshan Wang^{b,*}

^a Jiangsu Key Laboratory of Regional Resource Exploitation and Medicinal Research, School of Chemical Engineering, Huaiyin Institute of Technology, Huaian 223003, China

^b State Key Laboratory for the Chemistry and Molecular Engineering of Medicinal Resources, School of Chemistry and Pharmaceutical Sciences of Guangxi Normal University, Guilin 541004, China

^c Jiangsu Province Hi-Tech Key Laboratory for Biomedical Research, Southeast University, Nanjing 211189, China

^d Seasons Biotechnology (Taizhou) Co., Ltd, 21 Jiutiao Road, Jiaojiang District, Taizhou City, Zhejiang Province, 318000, China

ARTICLE INFO

Keywords:

Millepachine
Anti-cancer activity
Tubulin
Apoptosis

ABSTRACT

A new series of millepachine derivative containing aminophosphonate ester moieties were designed and synthesized, and evaluated for their anticancer activities using MTT assay. Among all the compounds, compound **9m** exhibited the most potent cytotoxic activity against all tested human cancer cell lines including multidrug resistant phenotype, which inhibited cancer cell growth with IC₅₀ values ranging from 0.85 to 3.09 μM, respectively. In addition, its low cytotoxicity toward human normal liver cells HL-7702 and sensitivity toward doxorubicin or cisplatin-resistant cells indicated the possibility for cancer therapy. Furthermore, **9m** significantly induced cell apoptosis and cell cycle arrest in G2/M phase and dramatically disrupted the microtubule organization. Moreover, a decrease in MMP, an increase in reactive oxygen species (ROS) generation and Bax/Bcl-2 ratio, accompanied by activated caspase-3 and -9, were observed in HepG-2 cells after incubation with **9m**, indicating that the mitochondrial pathway was involved in the **9m**-mediated apoptosis.

1. Introduction

Microtubules, as major components of the cytoskeleton, play critical roles in a series of fundamental cell functions, such as cell division and replication, cell signaling, cellular transport and motility [1–3]. Therefore, tubulin is recognized as important targets for anticancer drug development. Among antitumor agents, three major groups have been well characterized, the taxane site (e.g., paclitaxel and docetaxel) for microtubule-stabilizing agents, the vinca alkaloids site (e.g., vincristine, vinblastine, and vinorelbine), and the colchicine site (e.g., colchicine and CA-4) for microtubule polymerization inhibitors [4–7]. Unfortunately, drug resistance is one of the most important factors to restrict its chemotherapeutic efficacy in addition to the well-known serious side effects and poor solubility of these compounds. Thus, these have encouraged scientists to design and synthesize novel of anticancer agents for cancer therapy.

Chalcones, also known as α-β-unsaturated ketones, represent an important class of natural products, which received significant

attention for their pharmacological activities [8]. Chalcones have been reported for a broad spectrum of biological activities including antioxidant, anti-HIV, anti-inflammatory, anti-malarial and anti-cancer properties [8,9–11]. In addition, recent studies have indicated that most of chalcones and its analogues significantly induced apoptosis in a number of cell types [9,12–15]. In particular, millepachine (**1a**, Fig. 1), a novel chalcone with a 2, 2-dimethylbenzopyran motif, was first isolated from the *milletia pachycarpa* by Lijuan Chen group [16]. **1a** and its analogues (**1b**) have been found to exhibit the most potent cytotoxic activity against a variety of human cancer cell lines, which can inhibit strongly tubulin polymerization by binding to the colchicine site of tubulin, and effectively induce cells to arrest in the G2/M phase of the cell cycle [16,17]. However, the poor bioavailability and solubility render these substances suboptimum for clinical treatment of cancer. In an effort to further enhance the anticancer activity of millepachine, in our previous work, a series of **1a** derivative containing anilines were synthesized through the formation of amide bond in the presence of condensing agents, and evaluated their anti-proliferative activities

* Corresponding authors.

E-mail addresses: viphuangxc@126.com (X. Huang), zxliao@seu.edu.cn (Z. Liao), whengshan@163.com (H. Wang).

¹ Co-first author: These authors contributed equally to this work.

<https://doi.org/10.1016/j.bioorg.2019.103486>

Received 2 September 2019; Received in revised form 23 October 2019; Accepted 27 November 2019

0045-2068/© 2019 Published by Elsevier Inc.

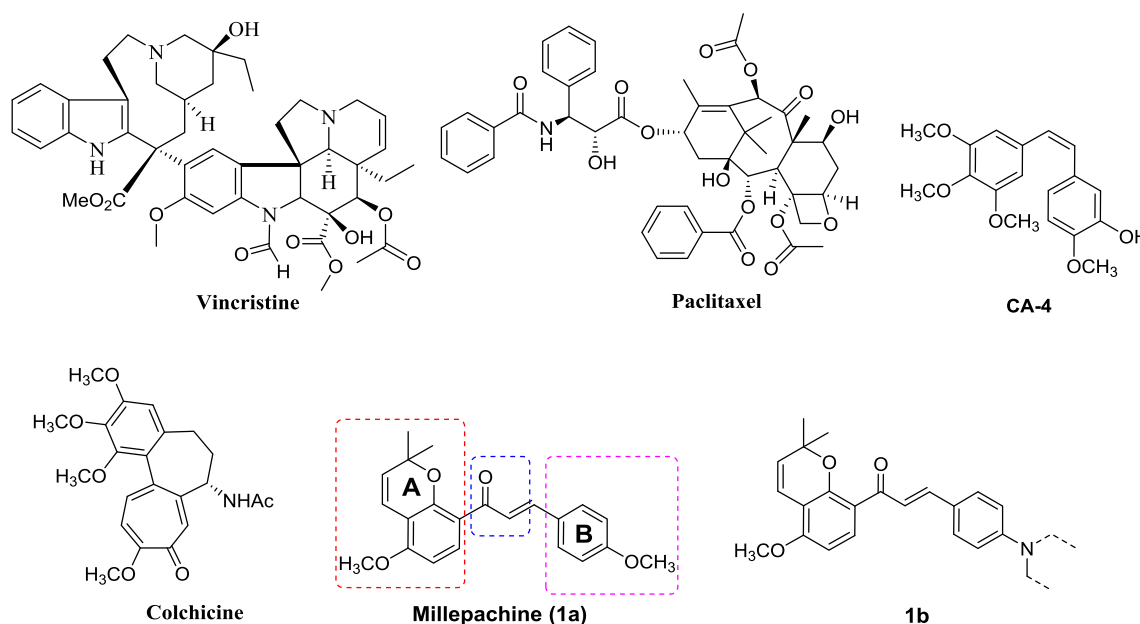


Fig. 1. Structures of natural products and millepachine analogs as potent inhibitors of tubulin polymerization.

[18]. However, the research results showed that most of the new derivatives exhibited equivalent or less potent cytotoxic activity against tested human cancer cells compared to **1a**. Recent studies have shown that introduction of a phosphate ester moiety to chemotherapy agents could obviously improve the solubility of drugs and increase transport through cellular membrane [19–21]. More importantly, many studies indicated that phosphate esters could be easily hydrolyzed under physiological conditions, suggesting introduction of aminophosphonate esters in drugs was an effective strategy to obtain targeted antitumor drugs [22–24]. In addition, most natural or synthetic aminophosphonate compounds have been found to exhibit moderate anticancer activity against a wide variety of cell lines [25–28]. Therefore, in order to obtain more effective compounds, we designed and synthesized a series of millepachine derivative containing aminophosphonate ester species at the *ortho*-position of methoxyl group on the B-ring.

In present study, a new series of millepachine derivative containing aminophosphonate ester moieties were synthesized and prepared as shown in Fig. 2. Furthermore, we characterized these target compounds and evaluated their *in vitro* anticancer activities as well as their mechanism of action. Compound **9m** exhibited the most potent anticancer activity against tested human cancer cell lines, with IC_{50} values ranging from 0.85 to 3.09 μ M, and also showed promising activities in drug-resistant tumor cells. The results of mechanistic experiments revealed that **9m** could significantly induce cell apoptosis, and strongly inhibit tubulin polymerization, and effectively induce cells to arrest in the G2/M phase of the cell cycle. Furthermore, our study further demonstrated that mitochondrial death pathway was involved in **9m** induced HepG-2 cells apoptosis through regulating the expression of Bcl-2 family proteins.

2. Results and discussion

2.1. Synthesis

The general steps to synthesize the target compounds **9a–9o** have been outlined in Fig. 2. Firstly, treatment of compound **1** with **2** in the presence of 1,8-Diazabicyclo[5.4.0]undec-7-ene (DBU) and catalytic amounts of $CuCl_2 \cdot 2H_2O$ proceeded easily to obtain intermediate **3**, and the resulting compound **3** was cyclized by heating in pyridine at 120 °C for overnight and we obtained the intermediate **4**. Secondly, by Claisen-

Schmidt condensation of **4** and **5** in the presence of KOH (50% w/v aqueous solution) in methanol at 0 °C for overnight to obtain the key intermediate **6**, and then treating with Fe powder and NH_4Cl in ethanol/water smoothly to obtain **7**. The key intermediate compounds **8a–8o** was prepared according to the reported procedures [20,23]. Finally, the final targets compounds **9a–9o** was obtained by the formation of amide bond between **7** and **8a–8o** in the presence of (2-(7-Azabenzotriazol-1-yl)-N, N', N'-tetramethyluroniumhexafluorophosphate) (HATU)/ Et_3N , respectively. The structures of these target compounds were confirmed by 1H NMR, ^{13}C NMR and high resolution mass spectra (HR-MS).

2.2. In vitro cytotoxicity

In order to searching for potential target compounds that displayed better activity, the reactions of millepachine analogue with different aminophosphonate ester species were performed to obtain title compounds **9a–9o**. The synthesized millepachine analogues were evaluated for their anti-proliferative activity against HepG-2 (hepatocellular), A375 (melanoma), K562 (leukemia) and NCI-H460 (lung) cancer cells and human normal liver cells HL-7702 using MTT assay. The cytotoxicities were expressed as IC_{50} values presented in Table 1. From the results of the MTT assay, it was noted that some of the synthesized new compounds (such as **9d**, **9g**, **9h**, **9j**, **9m**, **9n** and **9o**) were significantly more potent against the four cancer cell lines than that the parent compound **1a**. Especially, compound **9m** exhibited potent anticancer efficacy against the HepG-2, A375, K562, and NCI-H460 cancer cell lines, with IC_{50} values of 0.85, 2.03, 1.96, and 2.61 μ M, respectively. Among the tested compounds, with the exception of compounds **9e**, **9f**, **9k** and **9l**, the introduction of different substituent groups into the benzene ring of *para*-position or *meta*-position caused a significant increase in anti-proliferative efficacy relative to **9a** in the cancer cell lines. These results proved that *para*-position was better than *meta*-position. Interestingly, relative to **9b**, the introduction of $-OH$ group to the $-OCH_3$ group of *ortho*-position caused a 2.49- to 3.63-fold increase in the potency of compound **9m**. In addition, compound **9n**, the introduction of $-NO_2$ group to the $-OCH_3$ group of *ortho*-position, caused a significant increase in anti-proliferative efficacy relative to **9b** in the cancer cell lines, especially in K562 cells, where compound **9n** was 3.26-fold more potent than that of compound **9b** (8.21 μ M), with an

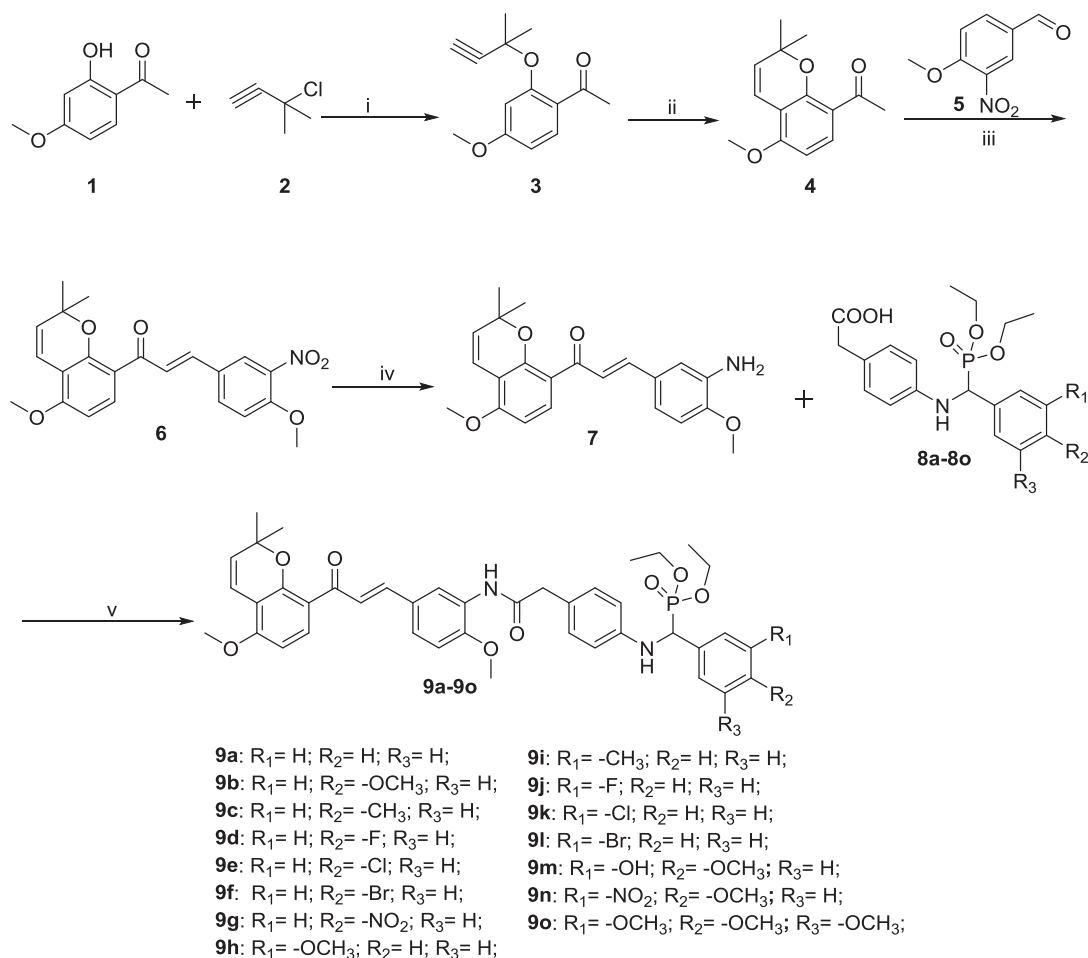


Fig. 2. Synthetic pathway to target compounds **9a–9o**. Reagents and conditions: (i) $\text{CuCl}_2 \cdot 2\text{H}_2\text{O}$, DBU, CH_3CN , 0°C , 5 h; (ii) Pyridine, 120°C , overnight; (iii) KOH (50% w/v aqueous solution), CH_3OH , 0°C , overnight; (iv) Fe, NH_4Cl , $\text{EtOH}/\text{H}_2\text{O}$, 85°C , 2 h; (v) HATU, Et_3N , Dimethyl formamide (DMF), 50°C , overnight.

IC_{50} value of $2.52 \mu\text{M}$, respectively. Moreover, compounds **9d** and **9j** were significantly more potent against the HepG-2, A375, K562, and NCI-H460 cancer cell lines than that of compound **9a**, but compounds **9e**, **9f**, **9k** and **9l** exhibited lower toxicity compared to **9a**. In shorts, the above results indicated that introduction of electron-donating groups

(such as $-\text{OCH}_3$ and $-\text{CH}_3$ group) or strong electron withdrawing groups (such as $-\text{F}$ and $-\text{NO}_2$ group) into the benzene ring of *para*-position or *meta*-position might be responsible for the enhanced anti-proliferative efficacy.

Table 1
Anti-proliferative activities of **9a–9o** against human cancer cell lines.

Compd.	IC_{50} (μM) ^a				
	HepG-2	A375	K562	NCI-H460	HL-7702
9a	6.26 ± 1.21	7.51 ± 1.24	10.36 ± 1.18	12.36 ± 1.63	> 20
9b	3.09 ± 1.17	5.06 ± 1.39	8.21 ± 1.23	7.25 ± 1.16	> 20
9c	5.22 ± 1.31	6.27 ± 1.42	6.23 ± 1.35	8.18 ± 1.51	> 20
9d	2.23 ± 1.09	3.26 ± 1.18	3.12 ± 1.33	4.66 ± 1.15	> 20
9e	18.39 ± 1.64	> 20	> 20	19.31 ± 1.81	> 20
9f	> 20	18.21 ± 1.66	> 20	> 20	> 20
9g	2.51 ± 1.22	3.38 ± 0.95	4.35 ± 1.01	5.27 ± 1.06	> 20
9h	5.33 ± 1.09	6.28 ± 1.47	10.72 ± 1.55	9.87 ± 1.83	> 20
9i	9.58 ± 1.73	10.96 ± 1.69	7.36 ± 1.83	9.82 ± 1.92	> 20
9j	4.87 ± 1.01	5.74 ± 1.22	6.71 ± 1.80	7.28 ± 1.07	> 20
9k	15.91 ± 1.76	> 20	> 20	> 20	> 20
9l	> 20	> 20	> 20	> 20	> 20
9m	0.85 ± 0.83	2.03 ± 0.91	1.96 ± 1.02	2.61 ± 1.13	> 20
9n	1.65 ± 0.94	3.07 ± 0.81	2.52 ± 1.06	3.02 ± 1.07	> 20
9o	4.84 ± 1.14	6.09 ± 1.29	5.30 ± 1.06	7.58 ± 1.44	> 20
1a ^b	5.35 ± 0.43	7.05 ± 0.72	8.58 ± 1.01	11.85 ± 1.08	> 20

^a Each data represents mean \pm S.D. from three different experiments performed in triplicate.

^b Used as positive controls.

Table 2
In vitro cell growth inhibitory effects of compound **9m** on drug resistant cells.

Compd.	IC ₅₀ (μM) ^a					
	MCF-7	MCF-7/DOX	RF ^b	A549	A549/CDDP	RF ^b
9m	1.75 ± 1.03	2.12 ± 1.15	1.24	3.09 ± 1.03	2.83 ± 1.64	0.92
DOX ^c	1.09 ± 0.91	43.5 ± 2.31	39.9	2.27 ± 1.15	2.95 ± 1.33	1.3
CDDP ^d	9.05 ± 1.67	15.21 ± 2.07	1.68	6.05 ± 1.46	27.36 ± 2.03	4.52

^a Each data represents mean ± S.D. from three different experiments performed in triplicate.

^b RF: Resistant factor = IC₅₀ of drug resistant cancer cell/ IC₅₀ of drug sensitive cancer cell.

^c Doxorubicin.

^d Cisplatin.

2.3. Effect of compound **9m** on multidrug resistant cells

Drug resistance has become a major problem for the first-line chemotherapy drugs [28,29]. For example, doxorubicin (DOX) resistant human breast carcinoma cells MCF-7/DOX, cisplatin (CDDP) resistant human lung cancer cells A549/CDDP. Therefore, to further investigate the selectivity of compound **9m** against a panel of parental and drug-resistant cancer cells, commercially available human breast carcinoma cells MCF-7, and the cell line MCF-7/DOX (doxorubicin resistant cells) and A549/CDDP (cisplatin resistant cell lines) were selected. The cytotoxicities were expressed as IC₅₀ values presented in Table 2. As shown in Table 2, although a high activity in parental cancer cell lines was exhibited, but the IC₅₀ value of DOX against MCF-7/DOX resistant cells was increased to 43.5 μM, respectively. It was noted that **9m** was not obviously changed for the DOX resistant cancer cells compared with DOX sensitive cells, with IC₅₀ values of 1.75 ± 1.03 μM and 2.12 ± 1.15 μM toward this pair of cancer cells, respectively. It was much significant to found that **9m** had a low resistance factor (1.24) compared to DOX (39.9). Interestingly, the similar trend was also observed in cisplatin resistant human lung cancer cells A549/CDDP. In shorts, these results suggested that **9m** displayed practically equally potent activities in the sensitive cells and the drug-resistant cells, indicating that **9m** might be useful in the treatment of drug refractory tumors.

2.4. Immunofluorescence staining of tubulin

In order to investigate the microtubule disrupting effects of the millepachine derivatives, we selected **9m** as a representative compound in a cell-based phenotypic screening. In present study, we determined the effect on the cellular microtubule network treated with 5 and 10 μM of **9m** for 24 h, and stained for α-tubulin (green) and DNA (blue) using confocal microscopy analysis. As shown in Fig. 3, confocal analysis of HepG-2 cells demonstrated a well-organized microtubule network in control cells in the absence of drug treatment, while cells treatment with 5 μM of **1a** displayed dramatically disrupted microtubule organization as expected. Notable, cells exposure to **9m** (5 and 10 μM) for 24 h significantly disrupted microtubule formation, respectively (Fig. 3). These morphological microtubules changes demonstrated that that **9m** exerted similar effects to millepachine (**1a**) on the microtubule network, indicating that **9m** was most likely targeting tubulin.

2.5. Compound **9m** inhibited the migration of HepG-2 cells in vitro

Recent studies have shown that microtubule targeting anticancer agents have been shown to be active against the cancer vasculature through inhibiting cell invasion and capillary tube formation [30]. Thus, in present study, the effect of **9m** on cell migration, which was a major mechanism involved in tumor invasion, was investigated through scratching a HepG-2 cells monolayer and monitoring the percentage of wound closure. As illustrated in Fig. 4, the wounds of HepG-2 cells displayed 63.5% closure in the absence of drug treatment after 24 h,

while the wounds of cells showed 53.6% closure after the cells exposure to **1a** (10 μM) for 24 h, respectively. Notably, the wounds of HepG-2 cells exhibited 51.5% and 38.6% after incubation of **9m** (5 and 10 μM) for 24 h, respectively (Fig. 4). Overall, these results suggested that **9m** significantly attenuated the migration of HepG-2 cells in a dose-dependent manner.

2.6. Compound **9m** induced apoptosis in HepG-2 cells

In recently, many studies revealed that most of anti-mitotic cancer agents exert their cytotoxic effects through apoptosis, thus we investigated features related to this pathway [9,16]. So, we investigated the occurrence of apoptosis in HepG-2 cells treated for 24 h with compound **9m** using a dual Annexin V staining/PI assay detected by flow cytometry. As shown in Fig. 5, after incubation with **9m** at the indicated concentrations (5 and 10 μM) for 24 h, the percentage of the early and late stage apoptosis cells were increased from 21.59 to 38.46%, but that of control group cells was only 3.85%. Moreover, the early and late stage apoptosis of HepG-2 cells treatment with **9m** increased gradually in a concentration-dependent manner. Notably, the 38.46% induction of HepG-2 cell apoptosis with incubation with 10 μM of **9m** was much higher than that of **1a** (17.18% apoptotic cells at the same concentration). Overall, these results indicated that **9m** effectively induced apoptosis in HepG-2 cancer cells.

2.7. Cell cycle analysis

It is well established that G2/M cell cycle arrest is strongly associated with inhibition of tubulin polymerization [31,32], thus the effect of **9m** on cell cycle were investigated in HepG-2 cells using PI-staining by flow cytometry analysis, and **1a** was served as a positive control. As illustrated in Fig. 6, untreated group cells as negative control exhibited 13.88% accumulation in G2/M phase, when HepG-2 cells were incubated with **1a** for 24 h, approximately 24.49% of the cells were arrested in G2/M phase as expected. Notably, the percentage of HepG-2 cells in the G2/M phase was 28.45% and 42.34% when the cells were treated with **9m** for 24 h at concentrations of 5 μM and 10 μM, respectively (Fig. 6). In shorts, the above results demonstrated that **9m** induce cancer cell cycle arrest at the G2/M phase in a concentration-dependent manner.

2.8. Compound **9m** triggered mitochondrial pathway dependent apoptosis

It is well known that mitochondria plays a crucial role in regulating cellular functions, and mitochondrial dysfunction has been proposed to be involved in triggering apoptosis [33,34]. Therefore, to further investigate if **9m** induced HepG-2 cells apoptosis was involved in a disruption of mitochondrial membrane integrity, the fluorescent probe JC-1 was used to detect the mitochondrial membrane potential (MMP) by flow cytometry analysis. As illustrated in Fig. 7, the MMP level in HepG-2 cells was decreased to 81.99% compared with the control group cells (94.76%) after exposure to 10 μM of **1a** for 24 h. Notably, incubation of

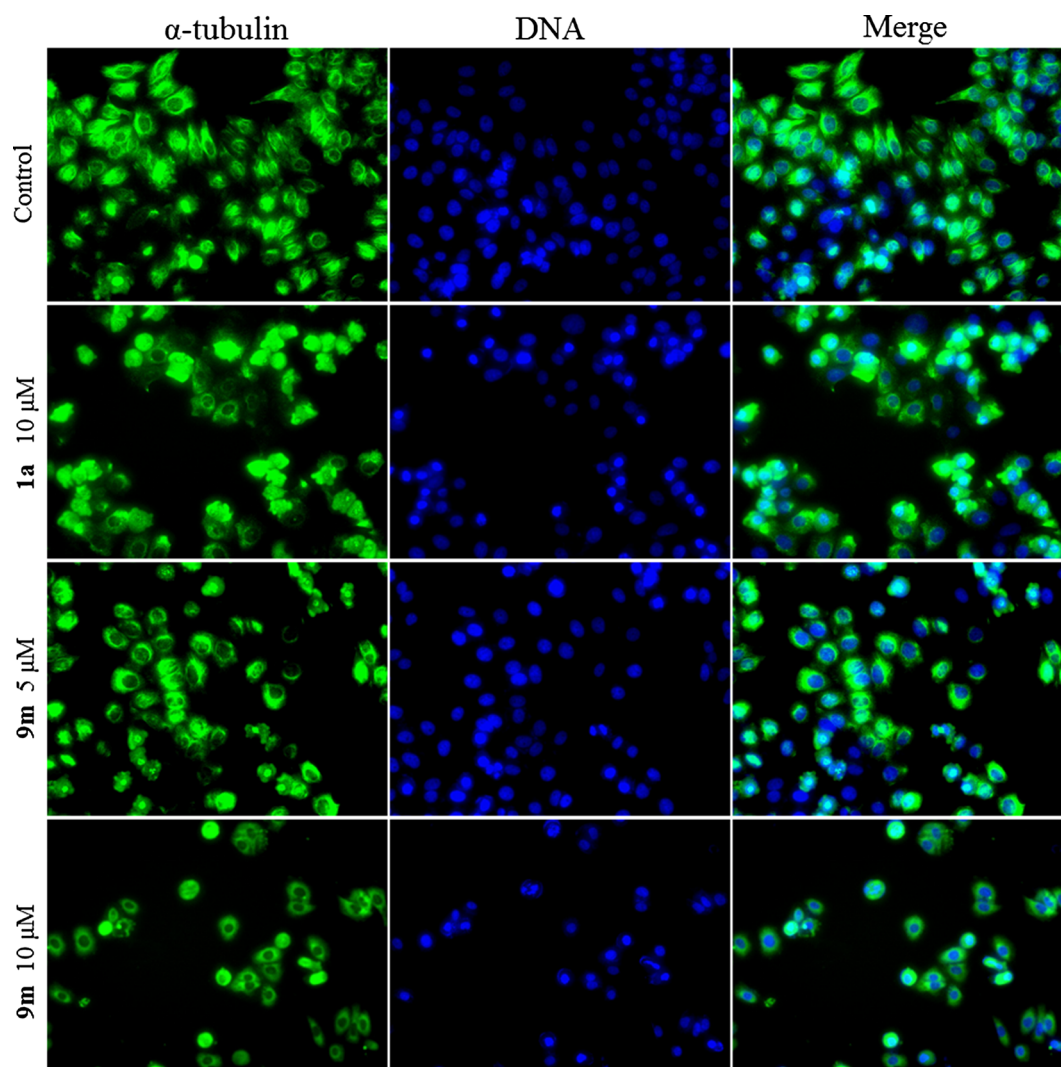


Fig. 3. Effects of **9m** on the microtubule network of cells. Untreated HepG-2 cells were served as negative control, and cells treated with **9m** (5 and 10 μM) for 24 h were fixed in methanol and stained with α -tubulin and counterstained with 4, 6-diamidino-2-phenylindole (DAPI). Millepachine (**1a**) was used as positive drug. Microtubules and unassembled tubulin are shown in green. DNA, stained with DAPI, was shown in blue. Data are expressed as the mean \pm SEM of three independent experiments.

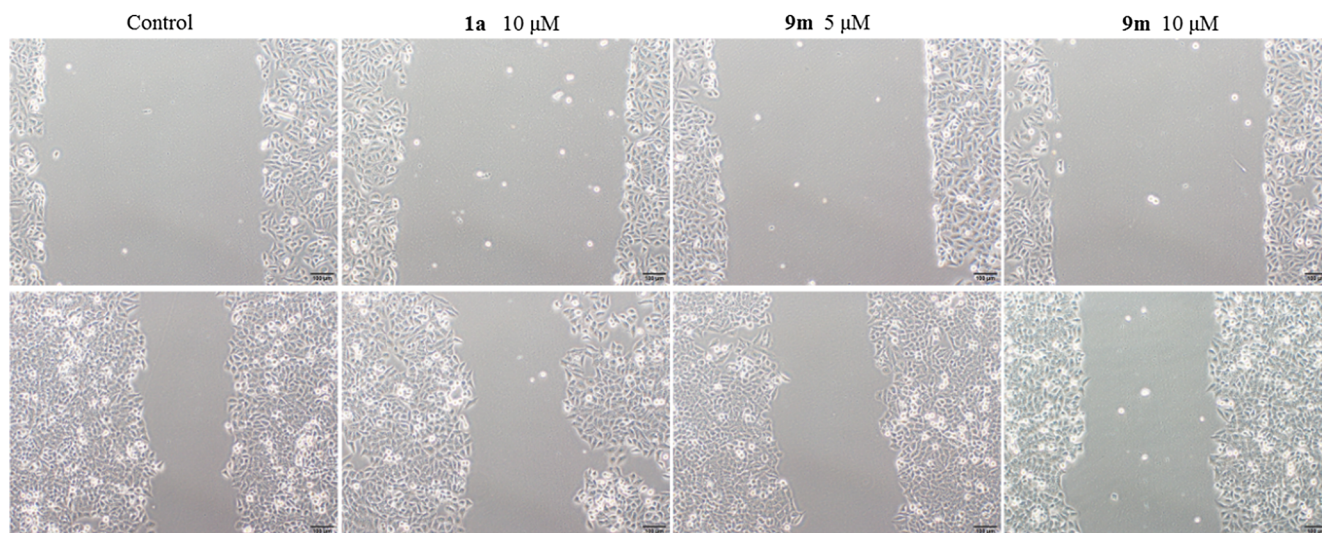


Fig. 4. Migration inhibition (wound-healing assay) of HepG-2 cells treated without or with the tested **9m** (5, 10 μM) and **1a** (10 μM) for 24 h at the indicated concentrations. Typical images were taken at 0 and 24 h. The widths of wounds are indicated with the lines (mm). Widths are statistically significant with $P < 0.05$.

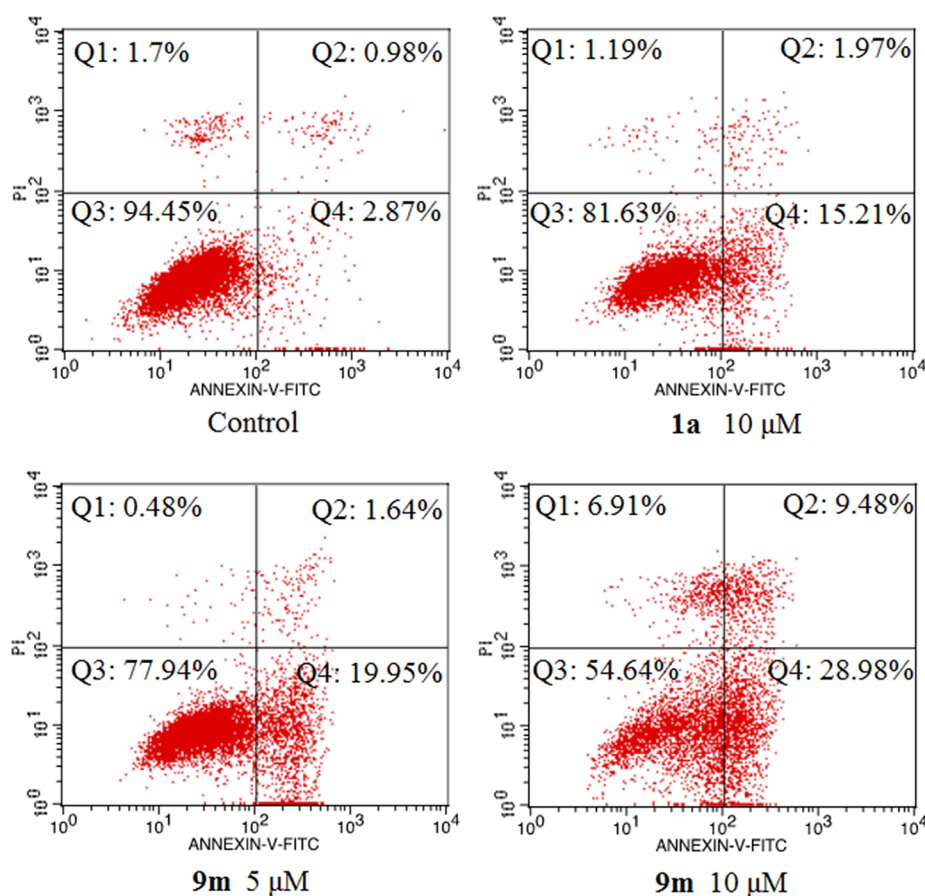


Fig. 5. Representative flow cytometric histograms of apoptotic HepG-2 cells after 24 h treatment with **9m** (5 and 10 μM) and **1a** (10 μM) as positive control. The cells were harvested and labeled with annexin-V-FITC and PI, and analyzed by flow cytometry. Q1, Q2, Q3, and Q4 represent four different cell states: necrotic cells, late apoptotic or necrotic cells, living cells and apoptotic cells, respectively. Data are expressed as the mean ± SEM for three independent experiments.

HepG-2 cells with **9m** (5 and 10 μM) induced the dissipation of MMP in a dose-dependent manner, the MMP level in HepG-2 cells was decreased to 80.86% and 61.59%, respectively (Fig. 7). In shorts, these results indicated that incubation of HepG-2 cells with **9m** cause a decrease the MMP level in a dose-dependent manner (Fig. 7), which demonstrated the activation of mitochondria mediated apoptosis.

2.9. Compound **9m** triggered ROS generation

Recent studies have shown that ROS generation was considered to play an important role in mitochondrial depolarization and apoptosis induction [35,36]. Therefore, we used the fluorescent probe 2', 7'-dichlorofluoresceindiacetate (DCFH-DA) to evaluate intracellular ROS levels in the presence or absence of **9m**. As illustrated in Fig. 8, after the HepG-2 cells exposure to 10 μM of **1a** for 24 h, the production of ROS level was enhanced to 16.76% compared with control group cells (1.06%). Notably, incubation of HepG-2 cells with **9m** (5 and 10 μM) induced the production of ROS level in a dose-dependent manner, the production of ROS level in HepG-2 cells was increased to 21.26% and 39.77%, respectively (Fig. 8). More importantly, when cells exposure to 10 μM of **9m**, the production of ROS level was more than two times that of **1a** (39.77% vs 16.76%), respectively. In short, these results indicated that ROS mediated apoptosis in HepG-2 cells incubated with **9m**.

2.10. Compound **9m** regulates the expression of apoptosis-related proteins

The above results demonstrated that **9m** induced HepG-2 cells apoptosis was closely related to the mitochondrial pathway. The Bcl-2 family proteins have been described as key regulators of MMP [37], as illustrated in Fig. 9, western blot analysis displayed that **9m** up-regulated the expression of Bax (pro-apoptosis Bcl-2 family protein), and suppressed the expression of Bcl-2 (anti-apoptosis Bcl-2 family protein).

Previously, many studies have indicated that the ratio of Bcl-2/Bax is decreased, resulting to the release of apoptogenic factors, such as cytochrome c [37]. Subsequently, cytochrome c further induced activation of caspase-3, and -9 [38]. Therefore, in the present study, to further investigate whether such a mechanism was involved in apoptosis induced by **9m**, the expression of cytochrome c, caspase-3 and -9 were determined by Western blot analysis. As shown in Fig. 9, the expression of cytochrome c, caspase-3 and -9 began to increase after incubation with **9m** for 24 h. These results indicated that mitochondrial death pathway was involved in **9m** induced HepG-2 cells apoptosis through regulating the expression of Bcl-2 family proteins.

3. Conclusions

In this study, a series of millepachine derivative containing aminophosphonate ester moieties were synthesized and evaluated their anticancer activities. Most of these synthesized compounds were significantly more potent than the parent molecule **1a** against both drug-sensitive and drug-resistant cancer cells. Especially, the most potent compound, **9m**, exhibited potent anticancer efficacy against the HepG-2, A375, K562, and NCI-H460 cancer cell lines, with IC₅₀ values of 0.85, 2.03, 1.96, and 2.61 μM, respectively. Notably, **9m** showed practically equally potent activities in the DOX or CDDP sensitive cells and resistant cells, and displayed low toxicity toward to human normal liver cells HL-7702. Moreover, flow cytometry analysis and immunofluorescence staining assay suggested that **9m** induced cell apoptosis and cell cycle arrest in G2/M phase through significantly inhibited microtubule polymerization. More importantly, the mitochondrial dysfunction and ROS overproduction up-regulated the expression of Bcl-2 family proteins, and then induced the mitochondrial release of certain cellular components, such as cytochrome c and triggered caspases family proteases such as caspase-3 and -9, finally leading to cell

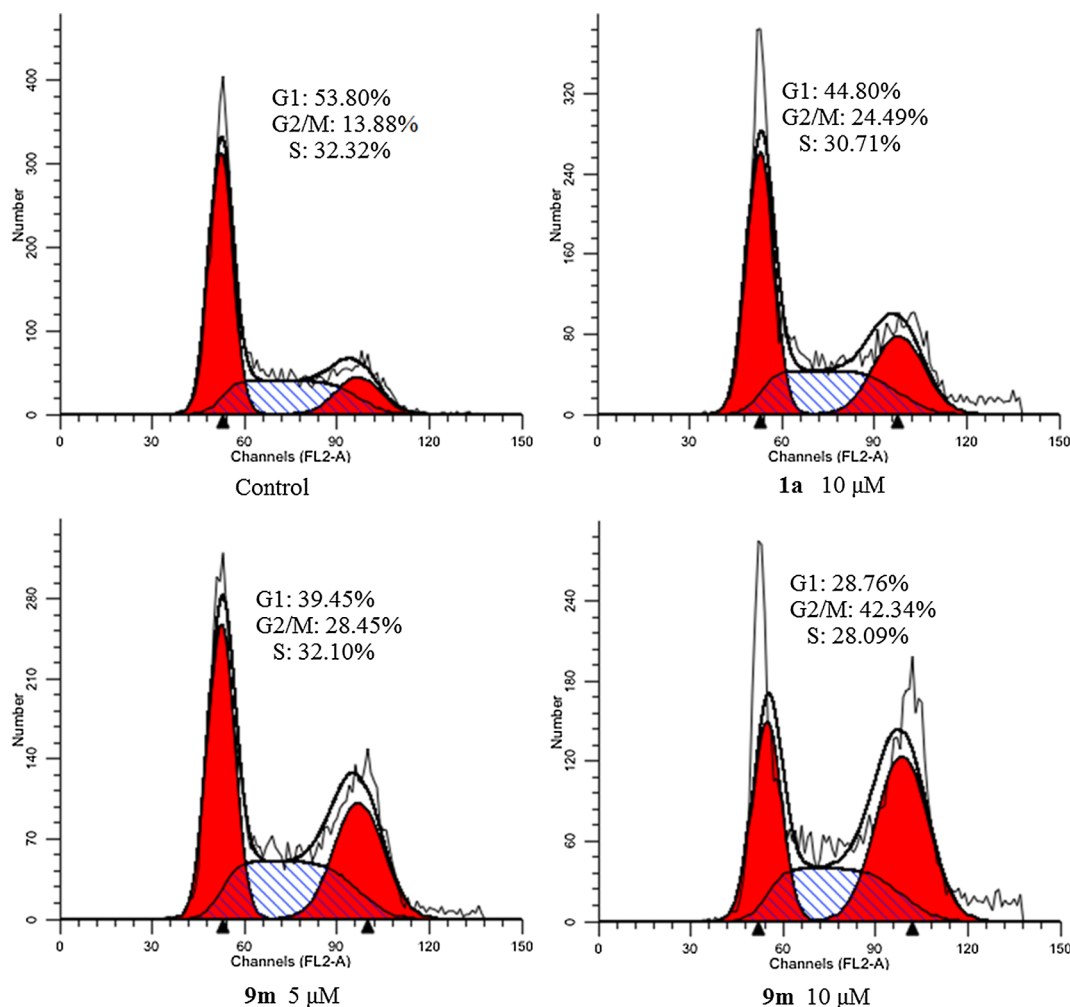


Fig. 6. Cell cycle arrest effect of **9m**. HepG-2 cells treated with **9m** (5 and 10 μM) and **1a** (10 μM) for 24 h. Then, the cells were trypsinized, harvested and washed three times with ice-PBS for PI-stained DNA content detected by flow cytometry.

apoptosis. In shorts, our results demonstrated that the newly developed millepachine analogue **9m** exhibited significant antitumor efficacy *in vitro*, and has the potential to be further developed into a promising antitumor compound for human cancers.

4. Experimental section

All chemicals and solvents were analytical reagent grade and commercially available, and used without further purification unless noted specifically. Column chromatography was performed using silica gel (200–300 mesh). Mass spectra were measured on an Agilent 6224 TOF LC/MS instrument. ^1H NMR and ^{13}C NMR spectra were recorded in CDCl_3 with a Bruker 400 or 600 MHz NMR spectrometer.

4.1. General procedure for the preparation of compounds **9a–9o**

Synthesis of compound 3. To a solution of compound **1** (8.3 g, 50.0 mmol) in dry CH_3CN (100 mL), $\text{CuCl}_2 \cdot 2\text{H}_2\text{O}$ (25 mg, 1.5 mmol), DBU (7.5 mL, 75.0 mmol) and 3-chloro-3-methyl-1-butyne (7.7 g, 75.0 mmol) were added at 0 $^\circ\text{C}$ and then the mixture reaction was stirred at the same temperature for 5 h, which was monitored by TLC. After completion of reaction for 5 h, the mixture was cooled at room temperature, then 2 N HCl (aq) was added to adjust pH = 2. After removing the solvent under reduced pressure, the residue was poured into water (500 mL) to yield yellow precipitate that was collected by filtration and washed with petroleum ether to obtain **3** as a yellow solid

(yield: 6.3 g, 75.9%) which was used directly without further purification. ^1H NMR (600 MHz, CDCl_3) δ 7.75 (d, J = 8.8 Hz, 1H), 7.18 (d, J = 2.3 Hz, 1H), 6.60–6.58 (m, 1H), 3.83 (s, 3H), 2.67 (s, 1H), 2.57 (s, 3H), 1.74 (s, 6H). HR-MS (m/z) (ESI): calcd for $\text{C}_{14}\text{H}_{16}\text{O}_3$ [$\text{M} + \text{H}$] $^+$: 233.1177; found: 233.1179.

Synthesis of compound 4. A solution of compound **3** (6.96 g, 30.0 mmol) in dry pyridine (120 mL) was stirred at 120 $^\circ\text{C}$ for overnight and monitored by TLC. After removing the solvent under reduced pressure, and then 2 N HCl (aq) was added to adjust pH = 2. The mixture was added dichloromethane (300 mL), washed with water, and the organic layer was dried over anhydrous Na_2SO_4 and concentrated under reduced pressure. The resulting crude product was purified by chromatography on silica gel eluted with petroleum ether/ethyl acetate to obtain compound **4** as a yellow oil (yield: 5.0 g, 71.8%). ^1H NMR (600 MHz, CDCl_3) δ 7.74 (d, J = 8.9 Hz, 1H), 6.66 (d, J = 10.0 Hz, 1H), 6.47 (d, J = 8.9 Hz, 1H), 5.61 (d, J = 10.0 Hz, 1H), 3.86 (s, 3H), 2.61 (s, 3H), 1.48 (s, 6H). HR-MS (m/z) (ESI): calcd for $\text{C}_{14}\text{H}_{16}\text{O}_3$ [$\text{M} + \text{Na}$] $^+$: 255.0997; found: 255.1001.

Synthesis of compound 6. A solution of 50% KOH (25 mL, aq) was added dropwise to a stirred solution of **4** (4.6 g, 12.92 mmol) and **5** (3.6 g, 12.92 mmol) in methanol (50 mL) at 0 $^\circ\text{C}$ and stirred at the same temperature for overnight. After completion of reaction, the mixture was poured into ice-water (300 mL), and adjusted to pH = 2–3 with con.HCl. The precipitated was filtered, washed with water and dried to offer the crude product which was purified by chromatography on silica gel eluted with petroleum ether/ethyl acetate to obtain compound **6** as

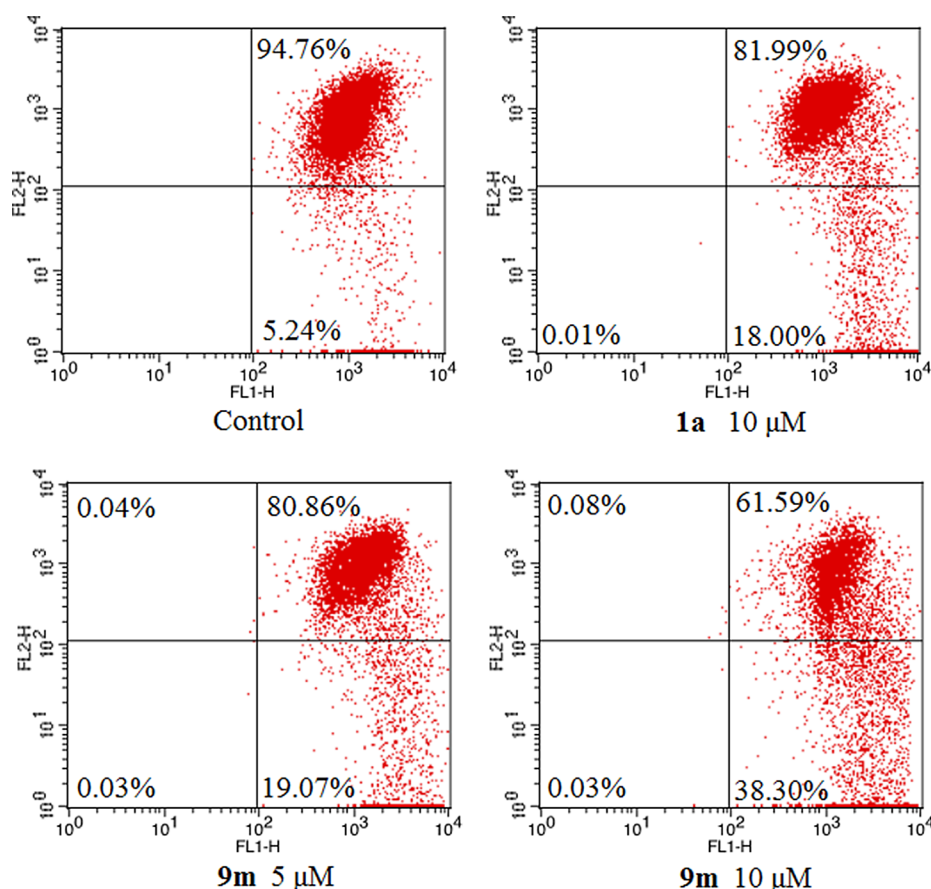


Fig. 7. Compound **9m** decreased the MMP of HepG-2 cells. The HepG-2 cells were treated with **9m** and **1a** at the indicated concentrations for 24 h followed by incubation with the fluorescence probe JC-1 for 30 min. Then, the cells were analyzed by flow cytometry. The experiments were performed three times, and the results of the representative experiments were shown.

a yellow solid (yield: 3.8 g, 74.5%). ^1H NMR (600 MHz, CDCl_3) δ 8.15 (d, $J = 2.1$ Hz, 1H), 7.75–7.73 (m, 2H), 7.71 (d, $J = 3.3$ Hz, 1H), 7.60 (d, $J = 15.7$ Hz, 1H), 7.12 (d, $J = 8.7$ Hz, 1H), 6.69 (d, $J = 10.0$ Hz, 1H), 6.53 (d, $J = 8.9$ Hz, 1H), 5.64 (d, $J = 10.0$ Hz, 1H), 4.00 (s, 3H), 3.89 (s, 3H), 1.51 (s, 6H). HR-MS (m/z) (ESI): calcd for $\text{C}_{22}\text{H}_{21}\text{NO}_6$ [$\text{M} + \text{H}$] $^+$: 396.1447; found: 396.1441.

Synthesis of compound **7**. To a solution of compound **6** (4.2 g, 10.46 mmol) in ethanol (60 mL)/water (5 mL) was added iron powder (3.6 g, 63.8 mmol) and NH_4Cl (342 mg, 6.4 mmol), and then the mixture stirred at 85 °C for 4 h. After completion of reaction, the mixture was cooled to room temperature and filtered through celite. The filter cake was washed with dichloromethane (100 mL), and concentrated under pressure. The residue was dissolved in CH_2Cl_2 (200 mL), washed with water. The organic layer dried over anhydrous Na_2SO_4 , filtered, and concentrated under reduced pressure. The crude product was purified by chromatography on silica gel eluted with $\text{CH}_2\text{Cl}_2/\text{CH}_3\text{OH}$ to obtain **7** as a yellow solid (yield: 3.45 g, 90.8%). ^1H NMR (600 MHz, CDCl_3) δ 7.68 (d, $J = 8.8$ Hz, 1H), 7.58 (d, $J = 15.7$ Hz, 1H), 7.52 (d, $J = 15.7$ Hz, 1H), 7.02–7.70 (m, 2H), 6.98 (d, $J = 2.0$ Hz, 1H), 6.79 (d, $J = 8.3$ Hz, 1H), 6.69 (d, $J = 10.0$ Hz, 1H), 6.50 (d, $J = 8.8$ Hz, 1H), 5.62 (d, $J = 10.0$ Hz, 1H), 3.88 (s, 3H), 3.87 (s, 3H), 1.50 (s, 6H). HR-MS (m/z) (ESI): calcd for $\text{C}_{22}\text{H}_{23}\text{NO}_4$ [$\text{M} + \text{H}$] $^+$: 366.1705; found: 366.1722.

4.1.1. Synthesis of target compound **9a**

To a solution of compound **8a** (124 mg, 0.329 mmol) in dry DMF (3 mL) was added HATU (156 mg, 0.411 mmol), Et_3N (57 μL , 0.411 mmol) and **7** (100 mg, 0.274 mmol), and stirred at 50 °C for overnight and monitored by TLC. The resulting mixture was stirred at room temperature for overnight and monitored by TLC. After completion of reaction, the mixture was diluted with CH_2Cl_2 (100 mL) and

washed with water (3 \times 200 mL), dried over anhydrous Na_2SO_4 and concentrated under pressure. The crude product which was purified by chromatography on silica gel eluted with $\text{CH}_2\text{Cl}_2/\text{CH}_3\text{OH}$ to give the target compound **9a** as a yellow solid (yield: 145 mg, 73.2%). ^1H NMR (600 MHz, CDCl_3) δ 8.72 (s, 1H), 7.77 (s, 1H), 7.70 (d, $J = 8.8$ Hz, 1H), 7.63 (s, 2H), 7.49 (s, 2H), 7.35 (t, $J = 7.6$ Hz, 2H), 7.29 (d, $J = 7.6$ Hz, 1H), 7.22–7.20 (m, 1H), 7.09 (d, $J = 8.4$ Hz, 2H), 6.77 (d, $J = 8.5$ Hz, 1H), 6.69 (d, $J = 10.0$ Hz, 1H), 6.65 (d, $J = 8.4$ Hz, 2H), 6.51 (d, $J = 8.9$ Hz, 1H), 5.64 (d, $J = 10.0$ Hz, 1H), 4.79 (d, $J = 24.4$ Hz, 1H), 4.17–4.11 (m, 2H), 3.97–3.89 (m, 1H), 3.89 (s, 3H), 3.70–3.66 (m, 1H), 3.61 (s, 3H), 3.60 (s, 2H), 1.54 (t, $J = 5.3$ Hz, 6H), 1.31 (t, $J = 7.1$ Hz, 3H), 1.13 (t, $J = 7.1$ Hz, 3H). ^{13}C NMR (150 MHz, CDCl_3) δ 190.15, 169.52, 158.24, 153.69, 149.28, 145.67, 145.57, 141.64, 135.77, 131.55, 130.44, 128.98, 128.72, 128.67, 128.10, 128.05, 127.86, 127.82, 125.85, 125.24, 124.00, 121.80, 117.78, 116.58, 114.29, 110.49, 109.87, 103.34, 63.46, 63.33, 56.46, 55.77, 55.73, 44.27, 27.95, 16.48, 16.23. HR-MS (m/z) (ESI): calcd for $\text{C}_{41}\text{H}_{45}\text{N}_2\text{O}_8\text{P}$ [$\text{M} + \text{Na}$] $^+$: 747.2811; found: 747.2818.

4.1.2. Synthesis of target compound **9b**

The compound **9b** was prepared from compound **8b** and compound **7** according to describe for **9a** method: 150 mg, 72.8% yield as a yellow solid; ^1H NMR (400 MHz, CDCl_3) δ 8.69 (s, 1H), 7.75 (s, 1H), 7.67 (d, $J = 9.7$ Hz, 1H), 7.61 (s, 2H), 7.38 (d, $J = 8.3$ Hz, 2H), 7.19 (d, $J = 8.4$ Hz, 1H), 7.06 (d, $J = 7.6$ Hz, 2H), 6.86 (d, $J = 7.9$ Hz, 2H), 6.75 (d, $J = 8.0$ Hz, 1H), 6.67 (d, $J = 10.0$ Hz, 1H), 6.62 (d, $J = 7.6$ Hz, 2H), 6.48 (d, $J = 8.1$ Hz, 1H), 5.61 (d, $J = 10.0$, 1.0 Hz, 1H), 4.71 (d, $J = 23.9$ Hz, 1H), 4.14–4.07 (m, 2H), 3.97–3.91 (m, 1H), 3.86 (s, 3H), 3.76 (s, 3H), 3.72–3.66 (m, 1H), 3.61 (s, 3H), 3.57 (s, 2H), 1.52 (s, 6H), 1.28 (t, $J = 7.0$ Hz, 3H), 1.13 (t, $J = 7.0$ Hz, 3H). ^{13}C NMR (100 MHz, CDCl_3) δ 190.14, 169.54, 159.41, 158.26, 153.70, 149.33,

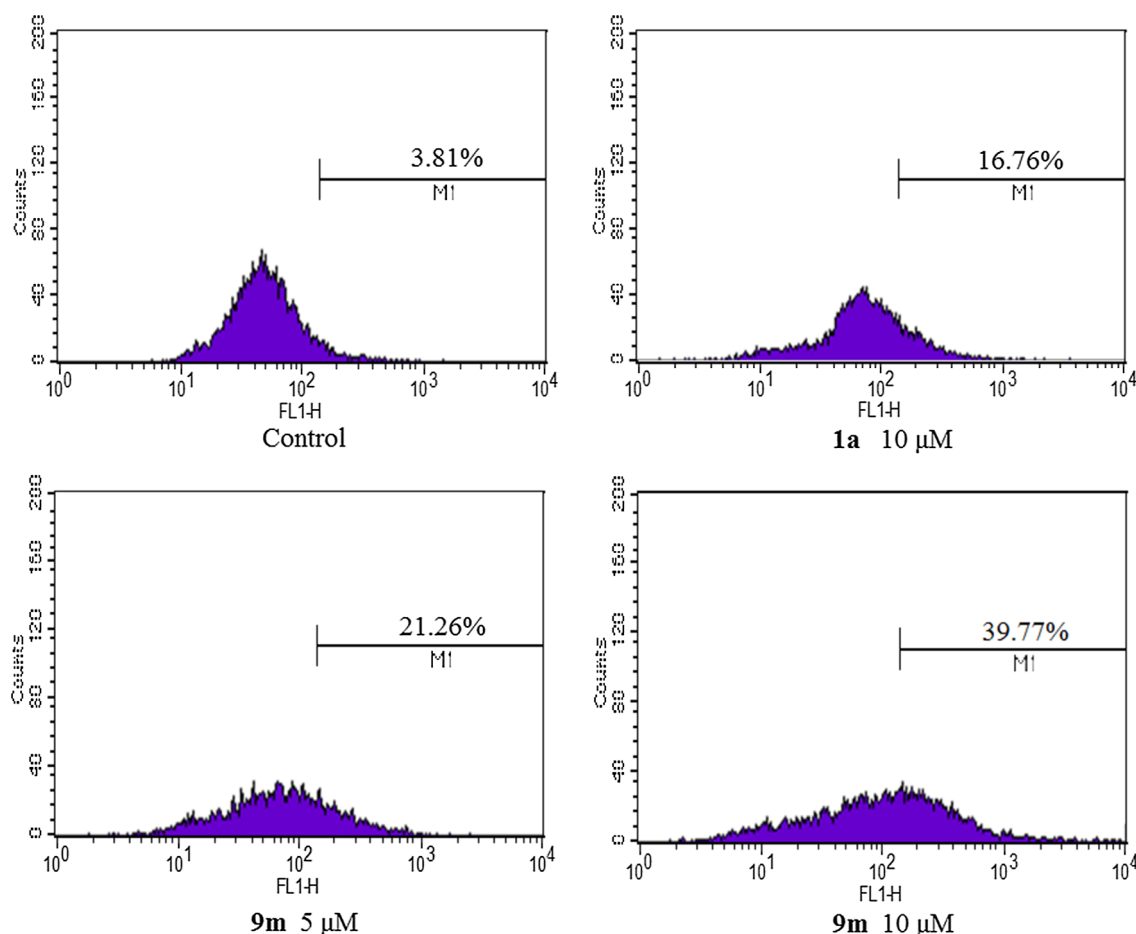


Fig. 8. Intracellular production of ROS by **9m** (5 and 10 μM) and **1a** (10 μM) following a 24 h incubation using 2', 7'-dichlorodihydrofluorescein diacetate (DCFH-DA) staining analysis by flow cytometry. The experiments were performed three times, and the results of the representative experiments were shown.

145.81, 145.66, 141.64, 131.55, 130.39, 129.00, 128.97, 128.16, 127.58, 125.93, 125.19, 123.99, 121.83, 117.89, 116.59, 114.37, 114.11, 110.52, 109.95, 103.36, 63.39, 63.27, 56.11, 55.76, 55.25, 44.27, 38.62, 27.95, 16.48, 16.29. HR-MS (m/z) (ESI): calcd for $\text{C}_{42}\text{H}_{47}\text{N}_2\text{O}_9\text{P}$ [$\text{M}+\text{Na}$] $^+$: 777.2917; found: 777.2909.

4.1.3. Synthesis of target compound **9c**

The compound **9c** was prepared from compound **8c** and compound **7** according to describe for **9a** method: 163 mg, 80.7% yield as a yellow solid; ^1H NMR (400 MHz, CDCl_3) δ 8.70 (s, 1H), 7.74 (s, 1H), 7.68 (d, $J = 8.8$ Hz, 1H), 7.61 (s, 2H), 7.36 (d, $J = 2.1$ Hz, 1H), 7.34 (d,

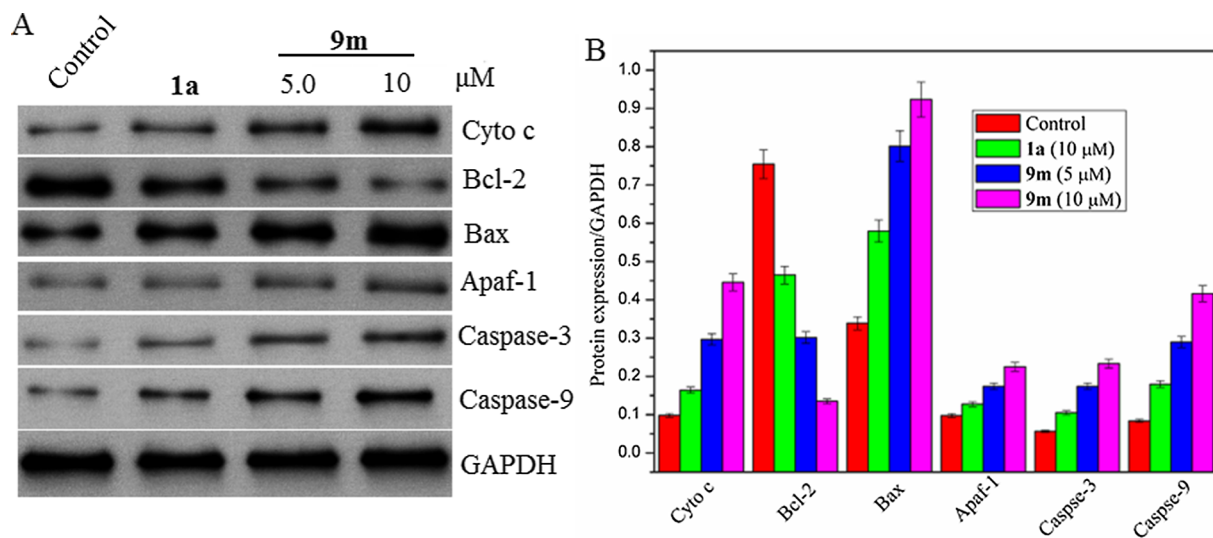


Fig. 9. HepG-2 cells were incubated with **9m** (5 and 10 μM) and **1a** (10 μM) for 24 h. (A) Representative Western blots of the effects of **9m** on the expression of apoptosis-related proteins. GAPDH was used as internal control. (B) Percentage expression levels of cytochrome c (Cyto c), Bcl-2, Bax, Apaf-1, caspase-3 and caspase-9. The percentage values are those relative to the GAPDH.

$J = 2.2$ Hz, 1H), 7.20–7.17 (m, 1H), 7.13 (d, $J = 8.0$ Hz, 2H), 7.06 (d, $J = 8.4$ Hz, 2H), 6.75 (d, $J = 8.5$ Hz, 1H), 6.67 (d, $J = 10.0$ Hz, 1H), 6.62 (d, $J = 8.5$ Hz, 2H), 6.48 (d, $J = 8.9$ Hz, 1H), 5.61 (d, $J = 10.0$ Hz, 1H), 4.73 (d, $J = 24.1$ Hz, 1H), 4.14–4.09 (m, 2H), 3.97–3.90 (m, 1H), 3.86 (s, 3H), 3.71–3.67 (m, 1H), 3.60 (s, 3H), 3.57 (s, 2H), 2.30 (s, 3H), 1.52 (s, 6H), 1.29 (t, $J = 7.1$ Hz, 3H), 1.12 (t, $J = 7.1$ Hz, 3H). ^{13}C NMR (100 MHz, CDCl_3) δ 190.12, 169.51, 158.25, 153.70, 149.31, 145.84, 145.69, 141.62, 137.73, 137.69, 132.66, 131.55, 130.40, 129.37, 128.97, 128.80, 128.17, 127.76, 127.71, 125.93, 125.18, 123.96, 121.84, 117.85, 116.59, 114.33, 110.51, 109.92, 103.35, 63.39, 63.26, 56.49, 55.76, 55.69, 44.28, 27.95, 21.12, 16.48, 16.26. HR-MS (m/z) (ESI): calcd for $\text{C}_{42}\text{H}_{47}\text{N}_2\text{O}_8\text{P}$ [$\text{M} + \text{Na}$] $^+$: 761.2968; found: 761.2977.

4.1.4. Synthesis of target compound 9d

The compound **9d** was prepared from compound **8d** and compound **7** according to describe for **9a** method: 149mg, 73.4% yield as a yellow solid; ^1H NMR (400 MHz, CDCl_3) δ 8.70 (s, 1H), 7.74 (s, 1H), 7.67 (d, $J = 8.8$ Hz, 1H), 7.61 (s, 2H), 7.47–7.43 (m, 2H), 7.20–7.18 (m, 2H), 7.07 (d, $J = 8.4$ Hz, 2H), 7.02 (t, $J = 8.6$ Hz, 2H), 6.76 (d, $J = 8.5$ Hz, 1H), 6.67 (d, $J = 10.0$ Hz, 1H), 6.59 (d, $J = 8.4$ Hz, 2H), 6.48 (d, $J = 8.9$ Hz, 1H), 5.61 (d, $J = 10.0$ Hz, 1H), 4.75 (d, $J = 24.1$ Hz, 1H), 4.15–4.09 (m, 2H), 3.99–3.95 (m, 1H), 3.86 (s, 3H), 3.79–3.71 (m, 1H), 3.64 (s, 3H), 3.58 (s, 2H), 1.52 (s, 6H), 1.29 (t, $J = 7.1$ Hz, 3H), 1.14 (t, $J = 7.1$ Hz, 3H). ^{13}C NMR (100 MHz, CDCl_3) δ 190.12, 169.41, 163.69, 161.27, 158.26, 153.69, 149.29, 145.53, 145.39, 141.60, 131.55, 130.43, 129.52, 129.38, 128.95, 128.82, 128.14, 125.96, 125.15, 124.31, 121.83, 117.96, 116.60, 115.73, 115.49, 114.30, 110.51, 109.96, 103.36, 63.41, 63.34, 56.13, 55.76, 55.73, 44.24, 27.95, 16.47, 16.26. HR-MS (m/z) (ESI): calcd for $\text{C}_{41}\text{H}_{44}\text{FN}_2\text{O}_8\text{P}$ [$\text{M} + \text{Na}$] $^+$: 765.2717; found: 765.2728.

4.1.5. Synthesis of target compound 9e

The compound **9e** was prepared from compound **8e** and compound **7** according to describe for **9a** method: 167 mg, 81.2% yield as a yellow solid; ^1H NMR (400 MHz, CDCl_3) δ 8.70 (s, 1H), 7.74 (s, 1H), 7.68 (d, $J = 8.8$ Hz, 1H), 7.61 (s, 2H), 7.47 (s, 1H), 7.37 (d, $J = 8.4$ Hz, 1H), 7.29 (d, $J = 7.9$ Hz, 2H), 7.21–7.18 (m, 1H), 7.08 (d, $J = 8.3$ Hz, 2H), 6.76 (d, $J = 8.5$ Hz, 1H), 6.67 (d, $J = 10.0$ Hz, 1H), 6.60 (d, $J = 8.4$ Hz, 2H), 6.49 (d, $J = 8.9$ Hz, 1H), 5.61 (d, $J = 10.0$ Hz, 1H), 4.96–4.84 (m, 1H), 4.73 (d, $J = 24.6$ Hz, 1H), 4.18–4.11 (m, 2H), 4.01–3.95 (m, 1H), 3.87 (s, 3H), 3.81–3.74 (m, 1H), 3.64 (s, 3H), 3.59 (s, 2H), 1.52 (s, 6H), 1.30 (t, $J = 7.1$ Hz, 3H), 1.15 (t, $J = 7.1$ Hz, 3H). ^{13}C NMR (100 MHz, CDCl_3) δ 190.14, 169.39, 158.25, 153.69, 149.29, 145.44, 145.29, 141.60, 138.29, 134.63, 131.55, 130.52, 129.92, 128.97, 128.83, 128.25, 128.14, 127.79, 126.06, 125.96, 125.18, 124.41, 121.84, 117.89, 116.60, 114.24, 110.51, 109.93, 103.35, 63.55, 63.48, 56.48, 55.76, 55.69, 44.25, 27.96, 16.45, 16.23. HR-MS (m/z) (ESI): calcd for $\text{C}_{41}\text{H}_{44}\text{ClN}_2\text{O}_8\text{P}$ [$\text{M} + \text{Na}$] $^+$: 781.2422; found: 781.2412.

4.1.6. Synthesis of target compound 9f

The compound **9f** was prepared from compound **8f** and compound **7** according to describe for **9a** method: 146 mg, 66.4% yield as a yellow solid; ^1H NMR (400 MHz, CDCl_3) δ 8.70 (s, 1H), 7.73 (s, 1H), 7.68 (d, $J = 8.8$ Hz, 1H), 7.61 (s, 2H), 7.46 (d, $J = 8.3$ Hz, 2H), 7.36 (d, $J = 2.1$ Hz, 1H), 7.34 (d, $J = 2.1$ Hz, 1H), 7.21–7.19 (m, 1H), 7.07 (d, $J = 8.3$ Hz, 2H), 6.77 (d, $J = 8.5$ Hz, 1H), 6.67 (d, $J = 10.0$ Hz, 1H), 6.58 (d, $J = 8.4$ Hz, 2H), 6.49 (d, $J = 8.9$ Hz, 1H), 5.61 (d, $J = 10.0$ Hz, 1H), 4.72 (d, $J = 24.5$ Hz, 1H), 4.15–4.08 (m, 2H), 4.01–3.95 (m, 1H), 3.87 (s, 3H), 3.81–3.75 (m, 1H), 3.63 (s, 3H), 3.58 (s, 2H), 1.52 (s, 6H), 1.29 (t, $J = 7.1$ Hz, 3H), 1.16 (t, $J = 7.1$ Hz, 3H). ^{13}C NMR (100 MHz, CDCl_3) δ 190.15, 169.38, 158.26, 153.69, 149.29, 145.41, 145.26, 141.61, 135.11, 131.80, 131.55, 130.47, 129.55, 128.96, 128.83, 128.12, 125.96, 125.17, 124.41, 121.98, 121.84, 116.61, 114.33, 110.52, 109.96, 103.36, 63.54, 63.47, 56.34, 55.77,

55.74, 44.25, 27.96, 16.47, 16.28. HR-MS (m/z) (ESI): calcd for $\text{C}_{41}\text{H}_{44}\text{BrN}_2\text{O}_8\text{P}$ [$\text{M} + \text{Na}$] $^+$: 827.1896; found: 827.1880.

4.1.7. Synthesis of target compound 9g

The compound **9g** was prepared from compound **8g** and compound **7** according to describe for **9a** method: 143 mg, 68.1% yield as a yellow solid; ^1H NMR (600 MHz, CDCl_3) δ 8.68 (s, 1H), 8.19 (d, $J = 8.5$ Hz, 2H), 7.73 (s, 1H), 7.67–7.65 (m, 3H), 7.60 (s, 2H), 7.20–7.19 (m, 1H), 7.08 (d, $J = 8.3$ Hz, 2H), 6.77 (d, $J = 8.5$ Hz, 1H), 6.66 (d, $J = 10.0$ Hz, 1H), 6.56 (d, $J = 8.4$ Hz, 2H), 6.48 (d, $J = 8.9$ Hz, 1H), 5.60 (d, $J = 10.0$ Hz, 1H), 4.87 (d, $J = 25.2$ Hz, 1H), 4.17–4.11 (m, 2H), 4.05–4.02 (m, 1H), 4.01–3.88 (m, 1H), 3.85 (s, 3H), 3.68 (s, 3H), 3.57 (s, 2H), 1.51 (s, 6H), 1.29 (t, $J = 7.1$ Hz, 3H), 1.18 (t, $J = 7.1$ Hz, 3H). ^{13}C NMR (150 MHz, CDCl_3) δ 190.15, 169.30, 158.26, 153.66, 149.21, 147.63, 145.50, 144.91, 143.98, 141.60, 131.54, 130.51, 128.93, 128.75, 128.68, 128.03, 125.90, 125.11, 124.85, 123.79, 121.76, 118.07, 116.60, 114.23, 110.48, 109.96, 103.36, 63.85, 63.61, 56.43, 55.78, 55.73, 44.17, 27.94, 16.48, 16.30. HR-MS (m/z) (ESI): calcd for $\text{C}_{41}\text{H}_{44}\text{N}_3\text{O}_{10}\text{P}$ [$\text{M} + \text{Na}$] $^+$: 792.2662; found: 792.2664.

4.1.8. Synthesis of target compound 9h

The compound **9h** was prepared from compound **8h** and compound **7** according to describe for **9a** method: 149mg, 72.3% yield as a yellow solid; ^1H NMR (600 MHz, CDCl_3) δ 8.73 (s, 1H), 7.78 (s, 1H), 7.71 (d, $J = 8.8$ Hz, 1H), 7.65 (s, 2H), 7.29–7.27 (m, 1H), 7.23–7.21 (m, 1H), 7.10 (d, $J = 8.2$ Hz, 2H), 7.07 (d, $J = 16.4$ Hz, 2H), 6.83 (d, $J = 8.2$ Hz, 1H), 6.78 (d, $J = 8.5$ Hz, 1H), 6.70 (d, $J = 10.0$ Hz, 1H), 6.66 (d, $J = 8.4$ Hz, 2H), 6.52 (d, $J = 8.8$ Hz, 1H), 5.65 (d, $J = 10.0$ Hz, 1H), 4.77 (d, $J = 24.3$ Hz, 1H), 4.19–4.14 (m, 2H), 4.00–3.96 (m, 1H), 3.90 (s, 3H), 3.80 (s, 3H), 3.74–3.70 (m, 1H), 3.64 (s, 3H), 3.62 (s, 2H), 1.56 (s, 6H), 1.31 (t, $J = 7.1$ Hz, 3H), 1.16 (t, $J = 7.1$ Hz, 3H). ^{13}C NMR (150 MHz, CDCl_3) δ 190.15, 169.53, 159.85, 158.24, 153.69, 149.29, 145.70, 145.60, 141.64, 137.40, 131.55, 130.44, 129.65, 128.98, 128.72, 128.11, 125.85, 125.24, 124.04, 121.80, 120.25, 117.77, 116.57, 114.31, 113.47, 113.42, 113.39, 110.49, 109.87, 103.33, 63.53, 63.36, 56.52, 55.77, 55.72, 55.24, 44.28, 27.95, 16.49, 16.26. HR-MS (m/z) (ESI): calcd for $\text{C}_{42}\text{H}_{47}\text{N}_2\text{O}_9\text{P}$ [$\text{M} + \text{Na}$] $^+$: 777.2917; found: 792.2907.

4.1.9. Synthesis of target compound 9i

The compound **9i** was prepared from compound **8i** and compound **7** according to describe for **9a** method: 138 mg, 68.8% yield as a yellow solid; ^1H NMR (600 MHz, CDCl_3) δ 8.69 (s, 1H), 7.74 (s, 1H), 7.68 (d, $J = 8.8$ Hz, 1H), 7.61 (s, 2H), 7.35 (d, $J = 1.9$ Hz, 1H), 7.34 (d, $J = 1.9$ Hz, 1H), 7.20–7.18 (m, 1H), 7.13 (d, $J = 7.9$ Hz, 2H), 7.05 (d, $J = 8.3$ Hz, 2H), 6.75 (d, $J = 8.5$ Hz, 1H), 6.67 (d, $J = 10.0$ Hz, 1H), 6.62 (d, $J = 8.4$ Hz, 2H), 6.49 (d, $J = 8.8$ Hz, 1H), 5.61 (d, $J = 10.0$ Hz, 1H), 4.73 (d, $J = 24.2$ Hz, 1H), 4.15–4.08 (m, 2H), 3.98–3.91 (m, 1H), 3.86 (s, 3H), 3.69–3.64 (m, 1H), 3.60 (s, 3H), 3.57 (s, 2H), 2.29 (s, 3H), 1.52 (s, 6H), 1.29 (t, $J = 7.0$ Hz, 3H), 1.12 (t, $J = 7.1$ Hz, 3H). ^{13}C NMR (150 MHz, CDCl_3) δ 190.18, 169.57, 158.26, 153.70, 149.30, 145.78, 145.68, 141.65, 137.75, 132.60, 131.56, 130.42, 129.38, 128.99, 128.76, 128.13, 127.75, 125.89, 125.24, 123.92, 121.82, 117.82, 116.59, 114.33, 110.50, 109.90, 103.35, 63.41, 63.28, 56.19, 55.77, 55.69, 44.28, 27.95, 21.15, 16.48, 16.26. HR-MS (m/z) (ESI): calcd for $\text{C}_{42}\text{H}_{47}\text{N}_2\text{O}_8\text{P}$ [$\text{M} + \text{Na}$] $^+$: 761.2968; found: 761.2973.

4.1.10. Synthesis of target compound 9j

The compound **9j** was prepared from compound **8j** and compound **7** according to describe for **9a** method: 129mg, 63.5% yield as a yellow solid; ^1H NMR (400 MHz, CDCl_3) δ 8.70 (s, 1H), 7.74 (s, 1H), 7.68 (d, $J = 8.8$ Hz, 1H), 7.61 (s, 2H), 7.34–7.28 (m, 2H), 7.19 (d, $J = 8.4$ Hz, 2H), 7.08 (d, $J = 8.3$ Hz, 2H), 6.96 (t, $J = 7.8$ Hz, 1H), 6.76 (d, $J = 8.4$ Hz, 1H), 6.67 (d, $J = 10.0$ Hz, 1H), 6.60 (d, $J = 8.3$ Hz, 2H), 6.48 (d, $J = 8.9$ Hz, 1H), 4.76 (d, $J = 24.6$ Hz, 1H), 4.18–4.08 (m, 2H),

4.02–3.96 (m, 1H), 3.86 (s, 3H), 3.81–3.72 (m, 1H), 3.64 (s, 3H), 3.59 (s, 2H), 1.52 (s, 6H), 1.29 (t, $J = 7.1$ Hz, 3H), 1.15 (t, $J = 7.1$ Hz, 3H). ^{13}C NMR (100 MHz, CDCl_3) δ 190.13, 169.41, 164.25, 161.83, 158.26, 153.69, 149.30, 145.48, 145.33, 141.61, 138.83, 131.55, 130.49, 130.20, 128.96, 128.81, 128.15, 125.95, 125.18, 124.38, 123.61, 121.84, 117.89, 116.60, 115.11, 114.87, 114.58, 114.27, 110.52, 109.94, 103.36, 63.51, 63.44, 56.51, 55.76, 55.75, 44.25, 27.95, 16.46, 16.24. HR-MS (m/z) (ESI): calcd for $\text{C}_{41}\text{H}_{44}\text{FN}_2\text{O}_8\text{P}$ [$\text{M} + \text{Na}$] $^+$: 765.2717; found: 765.2712.

4.1.11. Synthesis of target compound 9k

The compound **9k** was prepared from compound **8k** and compound **7** according to describe for **9a** method: 134 mg, 64.7% yield as a yellow solid; ^1H NMR (400 MHz, CDCl_3) δ 8.69 (s, 1H), 7.73 (s, 1H), 7.67 (d, $J = 8.8$ Hz, 1H), 7.61 (s, 2H), 7.42 (d, $J = 2.2$ Hz, 1H), 7.40 (d, $J = 2.3$ Hz, 1H), 7.30 (d, $J = 8.3$ Hz, 2H), 7.21–7.18 (m, 1H), 7.07 (d, $J = 8.4$ Hz, 2H), 6.76 (d, $J = 8.5$ Hz, 1H), 6.67 (d, $J = 10.0$ Hz, 1H), 6.58 (d, $J = 8.5$ Hz, 2H), 6.48 (d, $J = 8.9$ Hz, 1H), 5.61 (d, $J = 10.0$ Hz, 1H), 4.74 (d, $J = 24.5$ Hz, 1H), 4.15–4.10 (m, 2H), 4.01–3.95 (m, 1H), 3.86 (s, 3H), 3.80–3.74 (m, 1H), 3.63 (s, 3H), 3.58 (s, 2H), 1.52 (s, 6H), 1.29 (t, $J = 7.1$ Hz, 3H), 1.15 (t, $J = 7.1$ Hz, 3H). ^{13}C NMR (100 MHz, CDCl_3) δ 190.14, 169.39, 158.26, 153.69, 149.29, 145.44, 145.29, 141.61, 134.53, 133.86, 131.55, 130.46, 129.20, 129.15, 128.95, 128.82, 128.12, 125.96, 125.16, 124.38, 121.83, 117.96, 116.60, 114.32, 110.51, 109.96, 103.36, 63.52, 63.45, 56.26, 55.76, 55.73, 44.24, 38.61, 27.95, 16.47, 16.28. HR-MS (m/z) (ESI): calcd for $\text{C}_{41}\text{H}_{44}\text{ClN}_2\text{O}_8\text{P}$ [$\text{M} + \text{Na}$] $^+$: 781.2422; found: 781.2421.

4.1.12. Synthesis of target compound 9l

The compound **9l** was prepared from compound **8l** and compound **7** according to describe for **9a** method: 151 mg, 68.6% yield as a yellow solid; ^1H NMR (400 MHz, CDCl_3) δ 8.70 (s, 1H), 7.75 (s, 1H), 7.68 (d, $J = 8.8$ Hz, 1H), 7.63 (d, $J = 1.7$ Hz, 1H), 7.62 (s, 2H), 7.41 (t, $J = 6.7$ Hz, 2H), 7.22 (d, $J = 7.9$ Hz, 1H), 7.20–7.18 (m, 1H), 7.09 (d, $J = 8.3$ Hz, 2H), 6.76 (d, $J = 8.4$ Hz, 1H), 6.67 (d, $J = 10.0$ Hz, 1H), 6.61 (d, $J = 8.4$ Hz, 2H), 6.49 (d, $J = 8.8$ Hz, 1H), 5.62 (d, $J = 10.0$ Hz, 1H), 4.72 (d, $J = 24.5$ Hz, 1H), 4.18–4.09 (m, 2H), 4.02–3.94 (m, 1H), 3.87 (s, 3H), 3.81–3.73 (m, 1H), 3.64 (s, 3H), 3.59 (s, 2H), 1.52 (s, 6H), 1.30 (t, $J = 7.0$ Hz, 3H), 1.16 (t, $J = 7.1$ Hz, 3H). ^{13}C NMR (100 MHz, CDCl_3) δ 190.12, 169.39, 158.26, 153.69, 149.31, 145.43, 145.29, 141.61, 138.60, 131.55, 131.17, 130.76, 130.51, 130.20, 128.96, 128.80, 128.14, 126.50, 125.94, 125.18, 124.42, 122.80, 121.83, 117.89, 116.60, 114.24, 110.52, 109.94, 103.36, 63.56, 63.49, 56.44, 55.79, 55.76, 44.24, 27.96, 16.45, 16.23. HR-MS (m/z) (ESI): calcd for $\text{C}_{41}\text{H}_{44}\text{BrN}_2\text{O}_8\text{P}$ [$\text{M} + \text{Na}$] $^+$: 827.1896; found: 827.1887.

4.1.13. Synthesis of target compound 9m

The compound **9m** was prepared from compound **8m** and compound **7** according to describe for **9a** method: 127 mg, 60.4% yield as a yellow solid; ^1H NMR (400 MHz, CDCl_3) δ 8.69 (s, 1H), 7.75 (s, 1H), 7.67 (d, $J = 8.8$ Hz, 1H), 7.61 (s, 2H), 7.18–7.16 (m, 1H), 7.05 (d, $J = 7.5$ Hz, 3H), 6.95 (d, $J = 8.2$ Hz, 1H), 6.79 (d, $J = 8.3$ Hz, 1H), 6.74 (d, $J = 8.4$ Hz, 1H), 6.66 (d, $J = 10.0$ Hz, 1H), 6.62 (d, $J = 8.2$ Hz, 2H), 6.48 (d, $J = 8.9$ Hz, 1H), 5.61 (d, $J = 10.0$ Hz, 1H), 4.66 (d, $J = 24.0$ Hz, 1H), 4.16–4.08 (m, 2H), 3.98–3.92 (m, 1H), 3.86 (s, 3H), 3.83 (s, 3H), 3.75–3.67 (m, 1H), 3.62 (s, 3H), 3.57 (s, 2H), 1.52 (s, 6H), 1.29 (t, $J = 7.1$ Hz, 3H), 1.15 (t, $J = 7.1$ Hz, 3H). ^{13}C NMR (100 MHz, CDCl_3) δ 190.19, 169.62, 158.27, 153.71, 149.38, 146.55, 145.94, 145.85, 145.70, 141.69, 131.55, 130.39, 128.98, 128.74, 128.65, 128.15, 125.89, 125.24, 123.93, 121.82, 119.59, 117.84, 116.58, 114.38, 114.13, 110.82, 110.52, 109.93, 103.37, 63.48, 63.33, 56.24, 55.93, 55.76, 55.75, 44.26, 27.95, 16.47, 16.28. HR-MS (m/z) (ESI): calcd for $\text{C}_{42}\text{H}_{47}\text{N}_2\text{O}_{10}\text{P}$ [$\text{M} + \text{Na}$] $^+$: 793.2866; found: 793.2858.

4.1.14. Synthesis of target compound 9n

The compound **9n** was prepared from compound **8n** and compound **7** according to describe for **9a** method: 148 mg, 67.5% yield as a yellow solid; ^1H NMR (600 MHz, CDCl_3) δ 8.69 (s, 1H), 7.96 (s, 1H), 7.75 (s, 1H), 7.67 (d, $J = 8.7$ Hz, 2H), 7.60 (s, 2H), 7.20 (d, $J = 8.3$ Hz, 1H), 7.09 (d, $J = 8.0$ Hz, 2H), 7.07 (d, $J = 8.8$ Hz, 1H), 6.77 (d, $J = 8.4$ Hz, 1H), 6.67 (d, $J = 10.0$ Hz, 1H), 6.59 (d, $J = 8.0$ Hz, 2H), 6.49 (d, $J = 8.8$ Hz, 1H), 5.61 (d, $J = 10.0$ Hz, 1H), 4.75 (d, $J = 24.2$ Hz, 1H), 4.17–4.11 (m, 2H), 4.06–4.02 (m, 1H), 3.92 (s, 3H), 3.91–3.88 (m, 1H), 3.86 (s, 3H), 3.69 (s, 3H), 3.59 (s, 2H), 1.52 (s, 6H), 1.30 (t, $J = 7.1$ Hz, 3H), 1.20 (t, $J = 7.1$ Hz, 3H). ^{13}C NMR (150 MHz, CDCl_3) δ 190.15, 169.35, 158.25, 153.67, 152.66, 149.27, 145.11, 145.01, 141.62, 139.53, 133.34, 131.55, 130.53, 128.96, 128.73, 128.46, 128.05, 125.88, 125.17, 124.93, 124.71, 121.78, 117.99, 116.59, 114.28, 113.85, 110.48, 109.95, 103.35, 63.78, 63.58, 56.63, 55.81, 55.78, 55.34, 44.22, 27.95, 16.49, 16.34. HR-MS (m/z) (ESI): calcd for $\text{C}_{42}\text{H}_{46}\text{N}_2\text{O}_{11}\text{P}$ [$\text{M} + \text{Na}$] $^+$: 822.2768; found: 822.2764.

4.1.15. Synthesis of target compound 9o

The compound **9o** was prepared from compound **8o** and compound **7** according to describe for **9a** method: 159 mg, 71.3% yield as a yellow solid; ^1H NMR (400 MHz, CDCl_3) δ 8.69 (s, 1H), 7.76 (s, 1H), 7.66 (d, $J = 8.8$ Hz, 1H), 7.60 (s, 2H), 7.20–7.18 (m, 1H), 7.09 (d, $J = 8.3$ Hz, 2H), 6.76 (d, $J = 8.5$ Hz, 1H), 6.70 (d, $J = 2.2$ Hz, 2H), 6.65 (t, $J = 9.5$ Hz, 3H), 6.48 (d, $J = 8.9$ Hz, 1H), 5.61 (d, $J = 10.0$ Hz, 1H), 4.67 (d, $J = 24.0$ Hz, 1H), 4.15–4.09 (m, 2H), 4.00–3.91 (m, 1H), 3.86 (s, 3H), 3.83 (s, 6H), 3.80 (s, 3H), 3.76–3.70 (m, 1H), 3.64 (s, 3H), 3.59 (s, 2H), 1.51 (s, 6H), 1.29 (t, $J = 7.0$ Hz, 3H), 1.15 (t, $J = 7.1$ Hz, 3H). ^{13}C NMR (100 MHz, CDCl_3) δ 190.16, 169.47, 158.26, 153.67, 153.42, 149.29, 145.85, 145.71, 141.61, 137.74, 131.53, 131.44, 130.43, 128.94, 128.82, 128.14, 125.96, 125.12, 124.24, 121.82, 117.98, 116.60, 114.28, 110.51, 109.99, 104.88, 103.36, 63.45, 63.33, 60.84 (s), 57.11, 56.20, 55.76, 55.73, 44.26, 27.95, 16.50, 16.32. HR-MS (m/z) (ESI): calcd for $\text{C}_{44}\text{H}_{51}\text{N}_2\text{O}_{11}\text{P}$ [$\text{M} + \text{Na}$] $^+$: 837.3128; found: 837.3120.

4.2. In vitro cytotoxicity

In this study, all human cancer cell lines including HepG-2, A375, K562, NCI-H460, MCF-7, MCF-7/DOX, A549, A549/CDDP cancer cells and human normal liver cells HL-7702 using MTT assay were purchased from the Shanghai Cell Bank of the Chinese Academy of Sciences. Culture medium Roswell Park Memorial Institute (RPMI-1640), phosphate buffered saline (PBS, pH = 7.2), fetal bovine serum (FBS), and Antibiotic-Antimycotic came from KeyGen Biotech Company (China). All cancer cells were cultivate in the supplemented with 10% FBS, and human normal liver HL-7702 cells were cultivate in the supplemented with 20% FBS, 100 units/ml of penicillin and 100 g/ml of streptomycin in a humidified atmosphere of 5% CO_2 at 37 °C. Tested compounds were dissolved to stock concentrations of 2 mM with DMSO (Sigma); the lead compound **1a** used as a positive control, and the cytotoxicity of all target compounds against the tested cancer cells and human normal cells was investigated using MTT assay. All data were independently tested repeated in triplicate.

4.3. Immunofluorescence assay

HepG-2 cells were seeded in each well of six-well plates at the density of 0.5×10^5 cells/mL of the RPMI-1640 medium with 10% FBS to the final volume of 2 mL. Cells treated with **9m** (5.0 or 10 μM) and **1a** (10 μM) in a humidified atmosphere of 5% CO_2 at 37 °C for 24. After 24 h treatment, cells were fixed with 4% paraformaldehyde at 37 °C for 30 minutes, and then permeabilized with 0.5% Triton X-100/PBS for 15 minutes. After blocking for 30 minutes in 5% BSA/PBS, cells were washed with PBS and incubated with a-tubulin for 2 h, and then tubulin was immunostained with monoclonal antibody to a-tubulin followed by

fluorescence antibody. Cells were visualized by fluorescence microscope after the nuclei of cells were labeled with DAPI.

4.4. Cell wound-healing assay

HepG-2 cells were seeded in 6-well plates and allowed to grow to $\geq 95\%$ confluent. After being washed with thrice in PBS, and then wounds were created perpendicular to the lines by 20 μL tips, and unattached cells were removed by washing with thrice in PBS. Cells treated with **9m** (5.0 or 10 μM) and **1a** (10 μM) in a humidified atmosphere of 5% CO_2 at 37 $^\circ\text{C}$ for 24. After 24 h treatment, the cells were washed with thrice in PBS, and then photographed to mark the final scratched tracks. The migration rates analyzed by Equation 1: Migration rate (%) = $(d_1 - d_2)/d_1$. The d_1 and d_2 represented the width of wound at 0 and 24 h, respectively.

4.5. Cell apoptosis assay

HepG-2 cells were seeded in each well of six-well plates at the density of 0.5×10^5 cells/mL of the RPMI-1640 medium with 10% FBS to the final volume of 2 mL, and cells incubated for overnight in a humidified atmosphere of 5% CO_2 at 37 $^\circ\text{C}$. Cells treated with **9m** (5.0 or 10 μM) and **1a** (10 μM) in a humidified atmosphere of 5% CO_2 at 37 $^\circ\text{C}$ for 24. After 24 h incubation, cells were collected, washed thrice in PBS, and re-suspended in 120 μL of binding buffer at a final concentration of 0.5×10^6 cells/mL, and then cells were treated with 5 μL of annexin V-FITC and 5 μL of PI in the dark at 4 $^\circ\text{C}$ for 30 min, and examined by system software (Cell Quest; BD Biosciences).

4.6. Cell cycle assay

HepG-2 cells were seeded in each well of six-well plates at the density of 0.5×10^5 cells/mL of the RPMI-1640 medium with 10% FBS to the final volume of 2 mL, and cells incubated for overnight in a humidified atmosphere of 5% CO_2 at 37 $^\circ\text{C}$. Cells treated with **9m** (5.0 or 10 μM) and **1a** (10 μM) in a humidified atmosphere of 5% CO_2 at 37 $^\circ\text{C}$ for 24. After 24 h incubation, cells were collected, washed thrice in ice-PBS, fixed with ice-cold 70% ethanol at -20 $^\circ\text{C}$ for overnight. The cells were treated with 100 μg /mL RNase A for 30 min at 37 $^\circ\text{C}$ after washed thrice in ice-cold PBS, and finally stained with PI at 1 mg/ml in the dark at 4 $^\circ\text{C}$ for 30 min detected by flow cytometry.

4.7. Mitochondrial membrane potential (MMP) assay

HepG-2 cells were seeded in each well of six-well plates at the density of 0.5×10^5 cells/mL of the RPMI-1640 medium with 10% FBS to the final volume of 2 mL, and cells incubated for overnight in a humidified atmosphere of 5% CO_2 at 37 $^\circ\text{C}$. Cells treated with **9m** (5.0 or 10 μM) and **1a** (10 μM) in a humidified atmosphere of 5% CO_2 at 37 $^\circ\text{C}$ for 24. After 24 h treatment, cells were then stained with 2 μM JC-1 in the dark at room temperature for 30 min. After 30 min of incubation, cells were harvested at 2000 rpm and washed thrice in ice-PBS detected by flow cytometry.

4.8. Reactive oxygen species (ROS) assay

HepG-2 cells were seeded in each well of six-well plates at the density of 0.5×10^5 cells/mL of the RPMI-1640 medium with 10% FBS to the final volume of 2 mL, and cells incubated for overnight in a humidified atmosphere of 5% CO_2 at 37 $^\circ\text{C}$. Cells treated with **9m** (5.0 or 10 μM) and **1a** (10 μM) in a humidified atmosphere of 5% CO_2 at 37 $^\circ\text{C}$ for 24. After 24 h treatment, cells were then stained with DCFH-DA in the dark at 37 $^\circ\text{C}$ for 30 min. After 30 min of incubation, the cells were harvested at 2000 rpm and washed thrice in PBS detected by flow cytometry.

4.9. Western blot assay

Western blot analysis was performed as described previously [35]. HepG-2 cells were seeded in each well of six-well plates at the density of 0.5×10^5 cells/mL of the RPMI-1640 medium with 10% FBS to the final volume of 2 mL, and cells incubated for overnight in a humidified atmosphere of 5% CO_2 at 37 $^\circ\text{C}$. Cells treated with **9m** (5.0 or 10 μM) and **1a** (10 μM) in a humidified atmosphere of 5% CO_2 at 37 $^\circ\text{C}$ for 24. After incubation, cells were collected, centrifuged, and washed thrice in PBS. The pellet was then re-suspended in lysis buffer containing 150 mM NaCl, 50 mM Tris (pH 7.4), 1% (w/v) sodium deoxycholate, 1% (v/v) Triton X-100, 0.1% (w/v) SDS, and 1 mM EDTA (Beyotime, China). The lysates were incubated at 37 $^\circ\text{C}$ for 30 min, and centrifuged at 20000g at 4 $^\circ\text{C}$ for 10 min. The protein concentration in the supernatant was analyzed by the BCA protein assay reagents. Equal amounts of protein per line were separated on 12% SDS polyacrylamide gel electrophoresis and transferred to PVDF Hybond-P membrane (GE Healthcare). Membranes were incubated with 5% skim milk in Tris-buffered saline with Tween 20 (TBST) buffer for 1 h and then the membranes being gently rotated overnight at 4 $^\circ\text{C}$. Membranes were then incubated with primary antibodies against Cyto c, Bcl-2, Bax, Apaf-1, caspase-3, caspase-9 and PARP or GAPDH for overnight at 4 $^\circ\text{C}$. After three washes in TBST, the membranes were next incubated with peroxidase labeled secondary antibodies for 2 h. Then all membranes were washed with TBST four times for 20 min and the protein blots were detected by chemiluminescence reagent (Thermo Fischer Scientifics Ltd.). The X-ray films were developed with developer and fixed with fixer solution.

Declaration of Competing Interest

The authors declare that they have no known competing financial interests or personal relationships that could have appeared to influence the work reported in this paper.

Acknowledgements

We are grateful to the National Natural Science Foundation of China (Grant Nos. 21977021 and 81760626), and the Ministry of Education Innovation Team Fund (IRT_16R15, 2016GXNSFGA380005). The authors would also like to thank the Natural Science Foundation of Guangxi Province (AB17292075) and Guangxi Funds for Distinguished Experts, and the Key University Science Research Project of Jiangsu Province (18KJA360001) and the Postgraduate Research & Practice Innovation Program of Jiangsu Province (SJCX18-0899).

Appendix A. Supplementary material

Supplementary data to this article can be found online at <https://doi.org/10.1016/j.bioorg.2019.103486>.

References

- [1] M.A. Jordan, L. Wilson, Microtubules as a target for anticancer drugs, *Nat. Rev. Cancer*. 4 (2004) 253–265.
- [2] G. Attard, A. Greystoke, S. Kaye, J. De Bono, Update on tubulin-binding agents, *Pathol. Biol.* 54 (2006) 72–84.
- [3] L.A. Amos, What tubulin drugs tell us about microtubule structure and dynamics, *Semin. Cell Dev. Biol.* 22 (2011) 916–926.
- [4] Y.T. Wang, Y.J. Qin, N. Yang, Y.L. Zhang, C.H. Liu, H.L. Zhu, Synthesis, biological evaluation, and molecular docking studies of novel 1-benzene acyl-2-(1-methylindol-3-yl)-benzimidazole derivatives as potential tubulin polymerization inhibitors, *Eur. J. Med. Chem.* 99 (2015) 125–137.
- [5] M.A. Jordan, J.A. Hadfield, N.J. Lawrence, A.T. McGown, Tubulin as a target for anticancer drugs: agents which interact with the mitotic spindle, *Med. Res. Rev.* 18 (1998) 259–296.
- [6] P.B. Schiff, J. Fant, S.B. Horwitz, Promotion of microtubule assembly in vitro by taxol, *Nature*. 277 (1979) 665–667.
- [7] N.H. Nam, Combretastatin A-4 analogues as antimitotic antitumor agents, *Curr.*

- Med. Chem. 10 (2003) 1697–1722.
- [8] P. Singh, A. Anand, V. Kumar, Recent developments in biological activities of chalcones: a mini review, *Eur. J. Med. Chem.* 85 (2014) 758–777.
- [9] J. Yan, J. Chen, S. Zhang, J.H. Hu, L. Huang, X.S. Li, Synthesis, evaluation, and mechanism study of novel indole-chalcone derivatives exerting effective antitumor activity through microtubule destabilization *in vitro* and *in vivo*, *J. Med. Chem.* 59 (2016) 5264–5283.
- [10] H. Mirzaei, S. Emami, Recent advances of cytotoxic chalconoids targeting tubulin polymerization: Synthesis and biological activity, *Eur. J. Med. Chem.* 121 (2016) 610–639.
- [11] W. Cai, B. Zhang, D. Duan, J. Wu, J. Fang, Curcumin targeting the thioredoxin system elevates oxidative stress in HeLa cells, *Toxicol. Appl. Pharmacol.* 262 (2012) 341–348.
- [12] J. Chen, J. Yan, J. Hu, Y. Pang, L. Huang, X. Li, Synthesis, biological evaluation and mechanism study of chalcone analogues as novel anti-cancer agents, *RSC Adv.* 5 (2015) 68128–68135.
- [13] R. Schobert, B. Biersack, A. Dietrich, S. Knauer, M. Zoldakova, A. Fruehauf, T. Mueller, Pt(II) complexes of a combretastatin A-4 analogous chalcone: effects of conjugation on cytotoxicity, tumor specificity, and long-term tumor growth suppression, *J. Med. Chem.* 52 (2009) 241–246.
- [14] G.C. Wang, C.Y. Li, L. He, K. Lei, F. Wang, Y.Z. Pu, Z. Yang, D. Cao, L. Ma, J.Y. Chen, Y. Sang, X.L. Liang, M.L. Xiang, A.H. Peng, Y.Q. Wei, L.J. Chen, Design, synthesis and biological evaluation of a series of pyranochalcone derivatives containing indole moiety as novel anti-tubulin agents, *Bioorg. Med. Chem.* 22 (2014) 2060–2079.
- [15] D. Kumar, N.M. Kumar, K. Akamatsu, E. Kusaka, H. Harada, T. Ito, Synthesis and biological evaluation of indolyl chalcones as antitumor agents, *Bioorg. Med. Chem. Lett.* 20 (2010) 3916–3919.
- [16] W. Wu, H. Ye, L. Wan, X. Han, G. Wang, J. Hu, M. Tang, X. Duan, Y. Fan, S. He, L. Huang, H. Pei, X. Wang, X. Li, C. Xie, R. Zhang, Z. Yuan, Y. Mao, Y. Wei, L.J. Chen, Millepachine, a novel chalcone, induces G2/M arrest by inhibiting CDK1 activity and causing apoptosis via ROS-mitochondrial apoptotic pathway in human hepatocarcinoma cells *in vitro* and *in vivo*, *Carcinogenesis* 34 (2013) 1636–1643.
- [17] G.C. Wang, F. Peng, D. Cao, Z. Yang, X.L. Han, J. Liu, W.S. Wu, L. He, L. Ma, J.Y. Chen, Y. Sang, M.L. Xiang, A.H. Peng, Y.Q. Wei, L.J. Chen, Design, synthesis and biological evaluation of millepachine derivatives as a new class of tubulin polymerization inhibitors, *Bioorg. Med. Chem.* 21 (2013) 6844–6854.
- [18] X.C. Huang, R.Z. Huang, L.X. Li, S.H. Gou, H.S. Wang, Synthesis and biological evaluation of novel chalcone derivatives as a new class of microtubule destabilizing agents, *Eur. J. Med. Chem.* 132 (2017) 11–25.
- [19] F. Orsini, G. Sello, M. Sisti, Aminophosphonic acids and derivatives. Synthesis and biological applications, *Curr. Med. Chem.* 17 (2010) 264–289.
- [20] L. Jina, B. Zhang, S.X. Hua, M. Ji, X.C. Huang, R.Z. Huang, H.S. Wang, Glycyrrhetic acid derivatives containing aminophosphonate ester species as multidrug resistance reversers that block the NF- κ B pathway and cell proliferation, *Bioorg. Med. Chem. Lett.* 28 (2018) 3700–3707.
- [21] S.V. Zutphen, J. Reedijk, Targeting platinum antitumor drugs: Overview of strategies employed to reduce systemic toxicity, *Coord. Chem. Rev.* 249 (2005) 2845–2853.
- [22] S. Piccinonna, N. Margiotta, C. Pacifico, A. Denora, N.S. Fedi, M. Corsini, G. Natile, Dinuclear Pt(II)-bisphosphonate complexes: A scaffold for multinuclear or different oxidation state platinum drugs, *Dalton Trans.* 41 (2012) 9689–9699.
- [23] X.C. Huang, R.Z. Huang, S.H. Gou, Z.M. Wang, H.S. Wang, Anticancer platinum(IV) prodrugs containing monoaminophosphonate ester as a targeting group inhibit matrix metalloproteinases and reverse multidrug resistance, *Bioconjugate Chem.* 28 (2017) 1305–1323.
- [24] Z.Q. Xue, M. Lin, J. Zhu, J. Zhang, Y.Z. Li, Z.J. Guo, Platinum(II) compounds bearing bone-targeting group: Synthesis, crystal structure and antitumor activity, *Chem. Commun.* 46 (2010) 1212–1214.
- [25] K.B. Huang, Z.F. Chen, Y.C. Liu, Z.Q. Li, J.H. Wei, M. Wang, G.H. Zhang, H. Liang, Platinum(II) complexes with mono-aminophosphonate ester targeting group that induce apoptosis through G1 cell-cycle arrest: Synthesis, crystal structure and antitumor activity, *Eur. J. Med. Chem.* 63 (2013) 76–84.
- [26] X.C. Huang, M. Wang, Y.M. Pan, X.Y. Tian, H.S. Wang, Y. Zhang, Synthesis and antitumor activities of novel α -aminophosphonates dehydroabietic acid derivatives, *Bioorg. Med. Chem. Lett.* 23 (2013) 5283–5289.
- [27] K.B. Huang, Z.F. Chen, Y.C. Liu, Z.Q. Li, J.H. Wei, M. Wang, X.L. Xie, H. Liang, Platinum(II) complexes containing aminophosphonate esters: Synthesis, characterization, cytotoxicity and action mechanism, *Eur. J. Med. Chem.* 64 (2013) 554–561.
- [28] R. Brown, E. Curry, L. Magnani, C.S. Wilhelm-Benartzi, J. Borley, Poised epigenetic states and acquired drug resistance in cancer, *Nat. Rev. Cancer.* 14 (2014) 747–753.
- [29] S. Busschots, S. O'Toole, J.J. O'Leary, B. Stordal, Carboplatin and taxol resistance develops more rapidly in functional BRCA1 compared to dysfunctional BRCA1 ovarian cancer cells, *Exp. Cell Res.* 336 (2015) 1–14.
- [30] R. Kaur, G. Kaur, R.K. Gill, R. Soni, J. Bariwal, Recent developments in tubulin polymerization inhibitors: an overview, *Eur. J. Med. Chem.* 87 (2014) 89–124.
- [31] H. Chen, Y.M. Li, C.Q. Sheng, Z.L. Lv, G.Q. Dong, T.T. Wang, J. Liu, M.F. Zhang, L.Z. Li, T. Zhang, D.P. Geng, C.J. Niu, K. Li, Design and synthesis of cyclopropylamide analogues of combretastatin-A 4 as novel microtubule stabilizing agents, *J. Med. Chem.* 56 (2013) 685–699.
- [32] L.X. Li, X.C. Huang, R.Z. Huang, S.H. Gou, Z.M. Wang, H.S. Wang, Pt(IV) prodrugs containing microtubule inhibitors displayed potent antitumor activity and ability to overcome cisplatin resistance, *Eur. J. Med. Chem.* 156 (2018) 666–679.
- [33] K. Sinha, J. Das, P.B. Pal, P.C. Sil, Oxidative stress: the mitochondria-dependent and mitochondria-independent pathways of apoptosis, *Arch. Toxicol.* 87 (2013) 1157–1180.
- [34] M. Kamachi, T.M. Le, S.J. Kim, M.E. Geiger, P. Anderson, P.J. Utz, Human auto-immune sera as molecular probes for the identification of an autoantigen kinase signaling pathway, *J. Exp. Med.* 196 (2002) 1213–1225.
- [35] A. Zheng, H. Li, X. Wang, Z.H. Feng, J. Xu, K. Cao, B. Zhou, J. Wu, J.K. Liu, Anticancer effect of a curcumin derivative B63: ROS production and mitochondrial dysfunction, *Curr. Cancer Drug Targets* 14 (2014) 156–166.
- [36] S.H. Huang, L.W. Wu, A.C. Huang, C.C. Yu, J.C. Lien, Y.P. Huang, J.S. Yang, J.H. Yang, Y.P. Hsiao, W.G. Wood, C.S. Yu, J.G. Chung, Benzyl isothiocyanate (BITC) induces G2/M phase arrest and apoptosis in human melanoma A375.S2 cells through reactive oxygen species (ROS) and both mitochondria-dependent and death receptor-mediated multiple signaling pathways, *J. Agric. Food Chem.* 60 (2012) 665–675.
- [37] M.C. Wei, W.X. Zong, E.H.Y. Cheng, T. Lindsten, V. Panoutsakopoulou, A.J. Ross, K.A. Roth, G.R. MacGregor, C.B. Thompson, S.J. Korsmeyer, Proapoptotic Bax and Bak: a requisite gateway to mitochondrial dysfunction and death, *Science.* 292 (2001) 727–730.
- [38] Y. Gou, J. Wang, S.F. Chen, Z. Zhang, Y. Zhang, W. Zhang, F. Yang, α -Nheterocyclic thiosemicarbazone Fe(III) complex: Characterization of its antitumor activity and identification of anticancer mechanism, *Eur. J. Med. Chem.* 123 (2016) 354–364.